

D which imply that $F_n(z)$ is a hypergeometric function

$$F_n(z) \equiv F\left(-2n, 2+\beta+2n; \frac{3}{2}+(\beta/2); z\right)$$

To obtain the value of J_n , we shall use the fact that $F_n(z)$ is a Gegenbauer polynomial, since we have¹⁶

$$C_{2n}^\lambda(t) = \frac{(2\lambda + 2n - 1)!}{(2n)!(2\lambda - 1)!} F\left(2\lambda + 2n, -2n; \lambda + \frac{1}{2}, \frac{1-t}{2}\right)$$

which for $\lambda = 1 + \beta/2$ gives

$$F_n(z) = \frac{(1 + \beta)!(2n)!}{(2n + 1 + \beta)C_{2n}^{1+\beta/2}} (1 - 2z) \quad (\text{F-2})$$

Now, we consider the classical formula¹⁷

$$\int_{-1}^1 dt (1 - t^2)^{\lambda-1/2} [c_n^\lambda(t)]^2 = \frac{2^{-2\lambda}}{[(\lambda - 1)!]^2} \frac{2\pi(2\lambda + n - 1)!}{(n + \lambda)n!}$$

By setting $t = 1 - 2z$ and by choosing for λ the value $\lambda = 1/\beta/2$, we transform the preceding formula into

$$\int_0^1 dz z(1 - z)^{(1/2)+(\beta/2)} [C_{2n}^{1+\beta/2}(1 - 2z)]^2 = \frac{\pi 2^{-3-2\beta}}{\left[\left(\frac{\beta}{2}\right)!\right]^2} \frac{(2n + 1 + \beta)!}{\left(2n + 1 + \frac{\beta}{2}\right)!(2n)!} \quad (\text{F-3})$$

Finally, by combining eqs D-2 and D-3, we obtain the result

$$J_n = \frac{\pi 2^{-3-2\beta}}{\left[\left(\frac{\beta}{2}\right)!\right]^2} \frac{[(\beta + 1)!]^2 (2n)!}{\left(2n + 1 + \frac{\beta}{2}\right)!\left(2n + 1 + \frac{\beta}{2}\right)!} \quad (\text{F-4})$$

References and Notes

- (1) de Gennes, P.-G. *J. Chem. Phys.* **1971**, *55*, 572.

- (2) Doi, M.; Edwards, S. F. *J. Chem. Soc., Faraday Trans.* **1978**, *74*, 1789, 1802, 1818. *The Theory of Polymer Dynamics*; Clarendon Press; Oxford, 1986; Chapter 6.
- (3) Rubinstein, M.; Colby, R. *J. Chem. Phys.* **1988**, *89*, 5291.
- (4) Doi and Edwards already noted this fact in their book (see ref 2).
- (5) des Cloizeaux, J. *Europhys. Lett.* **1988**, *5*, 437 (note that in this paper, Figures 1 and 6 have been unduly permuted but not their captions). The double reptation concept is clearly formulated in this publication, but the same idea also appears in other papers: see discussion in section III.
- (6) Watanabe, H.; Kotaka, T. *Macromolecules* **1984**, *17*, 2316.
- (7) Watanabe, H.; Kotaka, T. *Macromolecules* **1987**, *20*, 530.
- (8) Marucci, G. *J. Polym. Sci., Polym. Phys. Ed.* **1985**, *23*, 159.
- (9) Viovy, J. L. *J. Phys. (Les Ulis, Fr.)* **1985**, *46*, 847. Rubinstein, M.; Helfand, E.; Pearson, D. S. *Macromolecules* **1987**, *20*, 822 (see also ref 2). Cassagnau, Ph. Thèse de Doctorat-Université de Pau et des Pays de l'Adour, 1988. Ball, R. C.; McLeish, T. C. B. *Macromolecules* **1989**, *22*, 1911.
- (10) Doi, M. *J. Polym. Sci. Lett.* **1981**, *19*, 265. Doi, M. *J. Polym. Sci., Polym. Phys. Ed.* **1983**, *21*, 667.
- (11) Kirkwood, J. G. *Selected Topics in Statistical Mechanics*; Zwanzig, R. W., Ed.; Gordon and Breach: London, 1967. *Selected Papers on Noise and Stochastic Processes*; Wax, N., Ed.; Dover: New York, 1954.
- (12) Titchmarsh, E. C. *The Theory of Functions*, 2nd ed.; Oxford University Press: London, 1939; Section 5.8, p 185.
- (13) Erdelyi, A., et al. *Higher Transcendental Functions*; McGraw-Hill: New York, 1953; Vol. I, Chapter II, p 56.
- (14) Gradshteyn, I. S.; Ryzhik, I. M. *Table of Integrals, Series and Products*; Academic Press: New York, 1965; pp 948, 950.
- (15) Jahnke, E.; Emde, F. *Tables of Functions*, 4th ed.; Dover: New York, 1945; p 11.
- (16) See ref 9, pp 1029 and 1030.
- (17) See ref 9, p 827.

Registry No. PBD, 9003-17-2.

Equilibrium Morphology of Block Copolymer Melts. 3

Kyozi Kawasaki* and Toshihiro Kawakatsu

Department of Physics, Faculty of Science, Kyushu University 33, Fukuoka 812, Japan

Received September 20, 1989; Revised Manuscript Received February 23, 1990

ABSTRACT: The field theoretical approach for block copolymer melts developed in our earlier work (Kawasaki, K.; et al. *Macromolecules* **1988**, *21*, 2972) was recast in such a way as to avoid power series expansion in the concentration variable. The general scaling behavior was found, which naturally gives rise to the well-known two-thirds power law of the domain size. The theory is related to other approaches by Helfand and co-workers and by Semenov. Numerical consequences of the theory are also presented that clearly demonstrate approach to the correct asymptotic behavior.

1. Introduction

In the first two of the present series to be referred to as OK¹ and KOK,² respectively, we have described attempts to extend Leibler's field theoretical formulation of block copolymer melts³ to include strong segregation regime in microphase-separated states. The free energy functional, $H[\psi]$, was obtained as a functional power series in the local order parameter field, $\psi(\mathbf{r})$. Despite the apparent success of OK in predicting the morphological phase diagram in the strong segregation region when the series was terminated in the fourth order, the higher order terms were found to contribute at least equally in KOK, and validity of the expansion was questioned. The present paper is motivated by our desire to find an alternate

approach free from the convergence question of the series expansion approach of OK and KOK.

We start from the formal field theoretical framework of KOK where the functional power series of $H[\psi]$ is divided into short-range and long-range contributions, the latter described in terms of the Gaussian chain statistics (section 2). Instead of expanding the long-range contribution in the power series as in KOK, we express it by introducing the field conjugate to $\psi(\mathbf{r})$, which is self-consistently determined for given $\psi(\mathbf{r})$ (section 3). In section 4 we derive the general scaling properties, a consequence of which is that the linear dimension of domains in microphase-separated states scales as two-thirds the power of the polymerization index in the strong segregation limit. The theory is applied to the lamellar phase in section 5 and

is related to the work of Helfand and co-workers.⁴ We also discuss the Semenov theory⁵ in section 6. Some numerical consequences of the theory are presented in section 7.

2. Summary of the Field Theoretic Formulation

Here we give a simplified version of the field theoretical formulation of a diblock copolymer melt. Details are referred to in KOK. We consider a system of a one-component AB block copolymer melt with the A-chain block ratio, f , described by the system Hamiltonian $\hat{H}(\hat{\mathbf{c}})$, where $\hat{\mathbf{c}}$ is the abbreviated notation for the chain configuration of the entire system. The molecular expression for the local order parameter, $\hat{\psi}(\mathbf{r})$, is defined as

$$\hat{\psi}(\mathbf{r}) = \sum_K^{A,B} f_K \hat{\rho}_K(\mathbf{r}) \quad (2.1)$$

with

$$f_A = 1 - f \quad f_B = -f \quad (2.2)$$

where $\hat{\rho}_K(\mathbf{r})$ denotes the molecular expression for the monomer number density of the species K . Upon introduction of the field $\phi(\mathbf{r})$ conjugate to $\hat{\psi}(\mathbf{r})$, the generating functional, $W\{\phi\}$, is defined in terms of the partition function, $Z\{\phi\}$, as

$$W\{\phi\} = T \ln [Z\{\phi\}/Z\{0\}] \quad (2.3)$$

with T the Boltzmann constant times the temperature and

$$Z\{\phi\} = \int d[\mathbf{c}] \exp[T^{-1}\{-\hat{H}(\mathbf{c}) + \int \phi(\mathbf{r}) \hat{\psi}(\mathbf{r}) d\mathbf{r}\}] \quad (2.4)$$

The integral is over all possible chain configurations of the entire system. The free energy functional, $H\{\psi\}$, expressed in terms of the average local order parameter, $\psi(\mathbf{r})$, is then obtained by Legendre transform as

$$H\{\psi\} = -W\{\phi\} + \int d\mathbf{r} \phi(\mathbf{r}) \psi(\mathbf{r}) \quad (2.5)$$

where $\phi(\mathbf{r})$ on the right-hand side is eliminated in favor of $\psi(\mathbf{r})$ through the relation

$$\delta W\{\phi\}/\delta \phi(\mathbf{r}) = \psi(\mathbf{r}) \quad (2.6)$$

One also readily verifies that

$$\delta H\{\psi\}/\delta \psi(\mathbf{r}) = \phi(\mathbf{r}) \quad (2.7)$$

$\psi(\mathbf{r})$ can be interpreted as the equilibrium average of $\hat{\psi}(\mathbf{r})$ in the presence of the field $\phi(\mathbf{r})$. $H\{\psi\}$ can be interpreted as the appropriate free energy in the equilibrium state with the external field, which maintains the average value $\psi(\mathbf{r})$ for $\hat{\psi}(\mathbf{r})$. The equilibrium order parameter profile in the absence of a conjugate field is then obtained, once $H\{\psi\}$ is known, by

$$\delta H\{\psi\}/\delta \psi(\mathbf{r}) = 0 \quad (2.8)$$

It is important to stress that (2.8) is not the result of any approximation like the mean-field theory since $H\{\psi\}$ is not the usual Ginzburg-Landau type free energy function despite its formal similarity. The major task for a theorist is to obtain $H\{\psi\}$. For $\phi = 0$ we see that $H\{\psi\}$ vanishes by its definition. Hence, $H\{\psi\}$ simply vanishes in an equilibrium state without the conjugate field. Thus the primary purpose of introducing $H\{\psi\}$ is to find the equilibrium average of $\hat{\psi}(\mathbf{r})$ where $\phi(\mathbf{r})$ can play the role of a symmetry-breaking field set equal to zero at the end. Alternatively, when $\psi(\mathbf{r})$ deviates from its equilibrium value in the absence of field, $\phi(\mathbf{r})$, which is not zero, serves as the thermodynamic driving force in the approach toward thermal equilibrium.

So far everything is general and formal. From now on we limit ourselves to the strong segregation regime (SSR) in which the system consists of well-defined A-rich and B-rich domains separated by narrow interfacial regions.⁴ Then the next crucial step is the assumed separation of $H\{\psi\}$ as

$$H\{\psi\} = H^S\{\psi\} + H^L\{\psi\} \quad (2.9)$$

This is motivated by the following consideration. Here we are dealing with a highly incompressible liquid with a clearly defined domain structure. This is characterized by fixed uniform monomer densities of the two species inside each domain. Such a state results in phase-separated binary liquids. In polymeric liquids such local properties can be modified by the local connectivity of monomers in chains. We suppose that $H^S\{\psi\}$ contains all the effects responsible for producing these local properties of the system. $H^S\{\psi\}$, in general, will assume very large values unless $\psi(\mathbf{r})$ is such that it corresponds to the well-defined domain structure mentioned above, which we denote by $\bar{\psi}(\mathbf{r})$. Since the total volume of A-rich domains (and hence of B-rich domains) is practically fixed in SSR when the total system volume, V , is given, the free energy, $H^S\{\bar{\psi}\}$, is concentrated in the interfacial region aside from an unimportant constant term, which will be omitted hereafter. Thus we take

$$H^S\{\bar{\psi}\} = \sigma A \quad (2.10)$$

where σ is the interfacial tension and A is the total area of interface for the state described by $\bar{\psi}(\mathbf{r})$.⁶

Now, the connectedness of a whole block copolymer molecule plays the decisive role in determining the morphology of the system composed of very long block copolymer chains where local microscopic details are not important. We assume that $H^L\{\psi\}$ takes care of this long-distance connectedness. Now, we invoke the so-called Flory theorem,⁸ saying that chain statistics of a very long polymer chain is asymptotically Gaussian in melts where excluded-volume interactions are screened out. Then all the effects of intersegmental interactions are included in H^S since A chains (B chains) can practically be found only in A domains (B domains), and we can use the model of non-interacting Gaussian chains to obtain $H^L\{\psi\}$, which will be denoted as $H_G\{\psi\}$. This was actually done in KOK where $H_G\{\psi\}$ was formally expanded as a functional power series in $\psi(\mathbf{r})$, whose coefficients are expressed in terms of the moments of $\hat{\psi}(\mathbf{r})$ obtained by Gaussian statistics of non-interacting block copolymer chains. We have noted that such an expansion quickly becomes prohibitively complicated and there is no sign of convergence.

In view of the prominent role played by the Flory theorem in this work, we discuss in Appendix A the screening of the excluded-volume interaction in a non-uniformly stretched situation as in block copolymers.

3. Evaluation of $H_G\{\bar{\psi}\}$ for Domain State

Since we are here dealing with noninteracting Gaussian chains, it is simpler to go back to (2.5) and to evaluate the expression on the right-hand side where W is replaced by W_G for Gaussian chains and ϕ is now written as ϕ_G . \hat{H} and $\hat{\psi}$ in (2.4) are simply the sum of contributions of each noninteracting Gaussian chain. Thus, denoting the contributions of chain 1 to \hat{H} and $\hat{\psi}$ by $\hat{H}_1(\mathbf{c}_1)$ and $\hat{\psi}_1$, respectively, where \mathbf{c}_1 denotes the conformation of chain 1, we obtain for the system of n chains

$$W_G\{\phi_G\} = n W_1\{\phi_G\} \quad (3.1)$$

$$W_1\{\phi_G\} = T \ln [Z_1\{\phi_G\}/Z_1\{0\}] \quad (3.2)$$

$$Z_1\{\phi_G\} = \int d\{\mathbf{c}_1\} \exp[T^{-1}\{-\hat{H}_1(\mathbf{c}_1) + \int d\mathbf{r} \phi_G(\mathbf{r}) \hat{\psi}_1(\mathbf{r})\}] \quad (3.3)$$

Here $\phi_G(\mathbf{r})$ is eliminated by the requirement

$$n\delta W_1\{\phi_G\}/\delta\phi_G(\mathbf{r}) = \psi(\mathbf{r}) \quad (3.4)$$

Needless to say that $\phi_G(\mathbf{r})$ obtained here, in general, differs from $\phi(\mathbf{r})$ obtained from (2.6) even when $\psi(\mathbf{r})$ is the same. A formal expression for $H_G\{\psi\}$, the Legendre transform of $W_G\{\phi_G\}$, in powers of $\psi(\mathbf{r})$ should yield the same result as obtained in KOK. In view of the complication and poor convergence of this expression, we prefer to evaluate $H_G\{\psi\}$ for an arbitrary domain structure described by $\bar{\psi}(\mathbf{r})$ numerically using (3.3) and (3.4) with $\psi(\mathbf{r}) = \bar{\psi}(\mathbf{r})$ and

$$H_G\{\bar{\psi}\} = -nW_1\{\phi_G\} + \int d\mathbf{r} \phi_G(\mathbf{r}) \bar{\psi}(\mathbf{r}) \quad (3.5)$$

For a Gaussian chain, \mathbf{c}_1 is a function $\mathbf{c}(t)$ where t is the chain contour running from 0 to N , the total chain contour length. Thus we take

$$\hat{H}_1(\mathbf{c}) = \hat{H}_1\{\mathbf{c}\} \equiv \frac{1}{2} \int_0^N dt \{\dot{\mathbf{c}}(t)\}^2 \quad (3.6)$$

with $\dot{\mathbf{c}}(t) \equiv d\mathbf{c}(t)/dt$, where the average of the squared distance between adjacent monomers in the absence of external potential was chosen to be $3T$. Then we have

$$\int d\mathbf{r} \phi_G(\mathbf{r}) \hat{\psi}_1(\mathbf{r}) = \int_0^N dt f(t) \phi_G(\mathbf{c}(t)) \quad (3.7)$$

with

$$\begin{aligned} f(t) &= f_A & 0 < t < N_A \equiv fN \\ f(t) &= f_B & N_A < t < N \end{aligned} \quad (3.8)$$

We now introduce the Helfand chain propagator,⁴ $Q_{tt'}(\mathbf{r}\mathbf{r}';\{\phi_G\})$, for $N > t \geq t' > 0$ by

$$Q_{tt'}(\mathbf{r}\mathbf{r}';\{\phi_G\}) \equiv \int_{\mathbf{c}_t=\mathbf{r}'}^{\mathbf{c}_t=\mathbf{r}} d\{\mathbf{c}\} \exp\left[T^{-1}\left\{\frac{1}{2}\int_{t'}^t ds \{\dot{\mathbf{c}}(s)\}^2 + \int_{t'}^t ds f(s) \phi_G(\mathbf{c}(s))\right\}\right] \quad (3.9)$$

which is normalized as

$$Q_{tt}(\mathbf{r}\mathbf{r}';\{\phi_G\}) = \delta(\mathbf{r}-\mathbf{r}') \quad (3.10)$$

This chain propagator is also obtained by solving the following differential equation under the condition of (3.10)

$$\frac{\partial}{\partial t} Q_{tt'}(\mathbf{r}\mathbf{r}';\{\phi_G\}) = \left[\frac{T}{2}\nabla^2 + T^{-1}f(t)\phi_G(\mathbf{r})\right] Q_{tt'}(\mathbf{r}\mathbf{r}';\{\phi_G\}) \quad (3.11)$$

We then find

$$Z_1\{\phi_G\}/Z_1\{0\} \equiv Z\{\phi_G\} \equiv \frac{1}{V} \int \int d\mathbf{r} d\mathbf{r}' Q_{NO}(\mathbf{r}\mathbf{r}';\{\phi_G\}) \quad (3.12)$$

where we have used

$$Z_1\{0\} = \int \int d\mathbf{r} d\mathbf{r}' Q_{NO}(\mathbf{r}\mathbf{r}';\{\phi_G\})|_{\{\phi_G\}=0} = V \quad (3.13)$$

which directly follows from (3.10) and (3.11). The equation for $\phi_G(\mathbf{r})$ for an arbitrary domain state $\bar{\psi}(\mathbf{r})$ is given from (3.4) as

$$\begin{aligned} \frac{n}{V} \frac{1}{Z\{\phi_G\}} \int \int d\mathbf{r}' d\mathbf{r}'' \int_0^N dt f(t) Q_{Nt}(\mathbf{r}'\mathbf{r}'';\{\phi_G\}) \times \\ Q_{t0}(\mathbf{r}\mathbf{r}'';\{\phi_G\}) = \bar{\psi}(\mathbf{r}) \end{aligned} \quad (3.14)$$

In SSR with narrow interfaces, the properties of the chain

propagator $Q_{tt'}(\mathbf{r}\mathbf{r}';\{\phi_G\})$ have been studied elsewhere^{4,9} and we here summarize the results where we write J for N_A :

$$(1) \quad J \geq t \geq t' \geq 0$$

$$Q_{tt'}(\mathbf{r}\mathbf{r}';\{\phi_G\}) = [\tilde{\rho}_A(\mathbf{r})\tilde{\rho}_A(\mathbf{r}')]^{1/2} \tilde{Q}_{tt'}^A(\mathbf{r}\mathbf{r}';\{\phi_G\}) \quad (3.15a)$$

$$(2) \quad N \geq t \geq t' \geq J$$

$$Q_{tt'}(\mathbf{r}\mathbf{r}';\{\phi_G\}) = [\tilde{\rho}_B(\mathbf{r})\tilde{\rho}_B(\mathbf{r}')]^{1/2} \tilde{Q}_{tt'}^B(\mathbf{r}\mathbf{r}';\{\phi_G\}) \quad (3.15b)$$

$$(3) \quad N \geq t \geq J \geq t' \geq 0$$

$$Q_{tt'}(\mathbf{r}\mathbf{r}';\{\phi_G\}) = [\tilde{\rho}_B(\mathbf{r})\tilde{\rho}_A(\mathbf{r}')]^{1/2} z_J \int_{\Sigma} d\mathbf{a} \tilde{Q}_{tJ}^B(\mathbf{r},\mathbf{r}(\mathbf{a});\{\phi_G\}) \times \tilde{Q}_{Jt'}^A(\mathbf{r}(\mathbf{a}),\mathbf{r}';\{\phi_G\}) \quad (3.15c)$$

We must now explain the notations. $\tilde{\rho}_K(\mathbf{r})$ is the local monomer density of the species K normalized to reduce to unity well inside the K -rich domain. Thus $\tilde{\rho}_K(\mathbf{r})$ vanishes well inside the K -poor domain in SSR. The quantity z_J , which is a measure of the interfacial width, is given by

$$z_J \equiv \int d\mathbf{n} \tilde{\rho}_A(\mathbf{n}) \tilde{\rho}_B(\mathbf{n}) \quad (3.16)$$

where the integral is over the coordinate \mathbf{n} normal to a small interfacial element. Note that the integrand is non-vanishing only in the interfacial region and the integral reduces to a constant. $\tilde{Q}_{tt'}^K(\mathbf{r}\mathbf{r}';\{\phi_G\})$ is defined only when both \mathbf{r} and \mathbf{r}' are inside the same K -rich domain and describes the propagator of a portion of the chain starting at \mathbf{r}' and t' and ending at \mathbf{r} and t in the same domain. This function is obtained by solving the following equation for $\mathbf{r}\mathbf{r}'$ inside the K -rich domain

$$\frac{\partial}{\partial t} \tilde{Q}_{tt'}^K(\mathbf{r}\mathbf{r}';\{\phi_G\}) = \left[\frac{T}{2}\nabla^2 + T^{-1}f_K\phi_G(\mathbf{r})\right] \tilde{Q}_{tt'}^K(\mathbf{r}\mathbf{r}';\{\phi_G\}) \quad (3.17)$$

under the conditions

$$\tilde{Q}_{tt}^K(\mathbf{r}\mathbf{r}';\{\phi_G\}) = \delta(\mathbf{r}-\mathbf{r}') \quad (3.18)$$

$$\mathbf{n}(\mathbf{a}) \cdot \nabla \tilde{Q}_{tt'}^K(\mathbf{r}\mathbf{r}';\{\phi_G\})|_{\mathbf{r} \rightarrow \mathbf{r}(\mathbf{a})} =$$

$$\mathbf{n}(\mathbf{a}) \cdot \nabla' \tilde{Q}_{tt'}^K(\mathbf{r}\mathbf{r}';\{\phi_G\})|_{\mathbf{r}' \rightarrow \mathbf{r}(\mathbf{a})} = 0 \quad (3.19)$$

where $\mathbf{n}(\mathbf{a})$ is the normal unit vector to the interface at \mathbf{a} and the gradient is evaluated as \mathbf{r} or \mathbf{r}' approaches the interface at \mathbf{a} from inside the domain in which the propagator is defined as is indicated. The integral in (3.15c) is over the interface Σ , which intersects the path from \mathbf{r}' to \mathbf{r} . (We should note that in contrast to the case of blend the integrals of $Q_{t0}^A(\mathbf{r},\mathbf{r}')$, etc., over \mathbf{r}' do not in general tend to $\rho_A(\mathbf{r})^{1/2}$, etc., even for sufficiently large t for block copolymers.) Using (3.15), we obtain, noting that $\bar{\psi}(\mathbf{r})$ is equal to $f_K\rho_0$ in the K -rich domain, ρ_0 being the total monomer density assumed to be uniform

$$H_G\{\bar{\psi}\} = -nT \ln Z + \rho_0 f_A \int_{\Omega_A} d\mathbf{r} \phi_G(\mathbf{r}) + \rho_0 f_B \int_{\Omega_B} d\mathbf{r} \phi_G(\mathbf{r}) \quad (3.20)$$

$$Z = \frac{z_J}{V} \int_{\Sigma_T} d\mathbf{a} \int_{\Omega_B(\mathbf{a})} d\mathbf{r} \int_{\Omega_A(\mathbf{a})} d\mathbf{r}' \tilde{Q}_{NJ}^B(\mathbf{r},\mathbf{r}(\mathbf{a})) \tilde{Q}_{J0}^A(\mathbf{r}(\mathbf{a}),\mathbf{r}') \quad (3.21)$$

where Z is the partition function of a single block copolymer chain spanning the interface. Here Ω_K is the sum of all the K -rich domains in the system and Σ_T is all the interfaces in the system. $\Omega_K(\mathbf{a})$ is the K -rich domain nearest to the interfacial element at \mathbf{a} (see Figure 1). The arguments $\{\phi_G\}$ are omitted in the \tilde{Q} 's for simplicity.

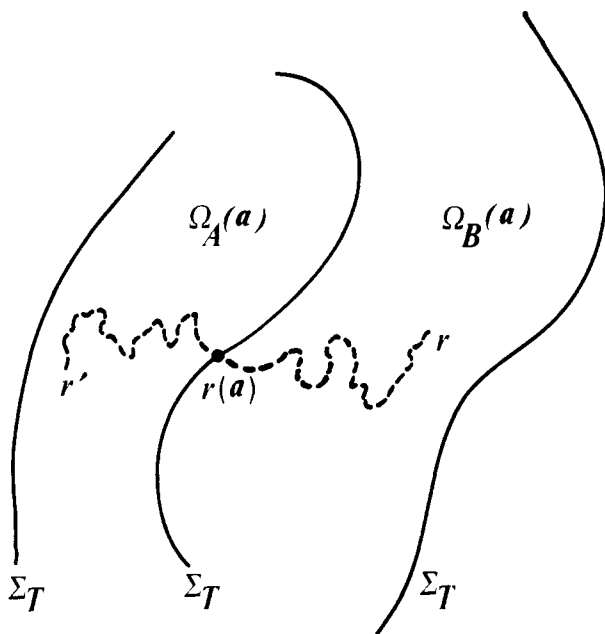


Figure 1. Illustration of the interfacial element at a and the two nearest domains that appear in (3.21). The dashed line is a block copolymer chain.

Equation 3.14 also reduces to the two equations

$$\frac{n}{V} \frac{z_J}{Z} \int_0^J dt f_A \int_{\Sigma(r)} da \int_{\Omega_B(a)} dr' \int_{\Omega_A(a)} dr'' \bar{Q}_{NJ}^B(r', r(a)) \times \bar{Q}_{Jt}^A(r(a), r) \bar{Q}_{t0}^A(r, r'') = \rho_0 f_A \quad \text{for } r \in \Omega_A \quad (3.22a)$$

$$\frac{n}{V} \frac{z_J}{Z} \int_0^J dt f_B \int_{\Sigma(r)} da \int_{\Omega_B(a)} dr' \int_{\Omega_A(a)} dr'' \bar{Q}_{NJ}^B(r', r) \times \bar{Q}_{tJ}^B(r, r(a)) \bar{Q}_{t0}^B(r(a), r'') = \rho_0 f_B \quad \text{for } r \in \Omega_B \quad (3.22b)$$

where $\Sigma(r)$ is the interface of the domain containing r . Equations 3.17–3.22 provide us with the complete recipe for evaluating $H_G\{\bar{\psi}\}$ where $\phi_G(r)$ is also determined up to an irrelevant arbitrary additive constant when the domain state $\bar{\psi}(r)$ is given. The arbitrariness of an additive constant for $\phi_G(r)$ is a consequence of the fact

$$\int \bar{\psi}(r) dr = \int \psi(r) dr = \int \bar{\psi}(r) dr = 0 \quad (3.23)$$

which does not depend on the SSR condition being satisfied. In SSR one can also verify directly that $\phi_G(r)$ for $r \in \Omega_K$ is arbitrary up to a constant ϕ_0^K , which can depend on K , where we note that $\bar{Q}_{t'K}$ acquires an arbitrary factor $\exp[f_K \phi_0^K \cdot (t-t')]$ and also that $nN = \rho_0 V$. We can then adjust the values of ϕ_0^K so that we have

$$\int_{\Omega_K} dr \phi_G(r) = 0 \quad \text{for } K = A \text{ and } B \quad (3.24)$$

With this choice we have simply

$$H_G\{\bar{\psi}\} = -nT \ln Z \quad (3.25)$$

4. Scaling

In view of heavy numerical work required to find the free energy $H\{\bar{\psi}\}$ in SSR even for the simplest kind of mesophases, i.e., the lamellar phase, it is very important to try to see possible general behavior like scaling. For this purpose we imagine changing the polymerization index, N , by a factor of λ and simultaneously changing the domain pattern by a length scale factor of γ , where we keep the total monomer density, ρ_0 , and the block ratio, f , fixed. Here we choose to keep the total number of chains n fixed so that the total volume, V^λ , after transformation becomes λV .

The quantities pertaining to the transformed state carry the superfixes λ anticipating that γ will ultimately depend on λ . Thus we have, for instance

$$\bar{\psi}^\lambda(r) = \bar{\psi}(r/\gamma) \quad (4.1)$$

First we take up the chain propagator after transformation, which satisfies

$$\frac{\partial}{\partial t} \bar{Q}_{t't''}^{K\lambda}(rr'; T; \{\phi_G^\lambda\}) = \left\{ \frac{T}{2} \nabla^2 + T^{-1} f_K \phi_G^\lambda(r) \right\} \bar{Q}_{t't''}^{K\lambda}(rr'; T; \{\phi_G^\lambda\}) \quad (4.2)$$

where the dependence of T was explicitly indicated, which will become necessary. We now explore a possibility of similarity where the transformed propagator is simply related to the untransformed one. Thus we make the ansatz

$$\bar{Q}_{t't''}^{K\lambda}(rr'; T; \{\phi_G^\lambda\}) = \gamma^{-3} \bar{Q}_{t/\lambda, t''/\lambda}^K(r/\gamma, r'/\gamma; T^\lambda; \{\phi_G\}) \quad (4.3)$$

where the factor γ^{-3} arises from the condition (3.10), which should remain invariant. The quantity T^λ is the transformed temperature to be determined now. Substituting (4.3) into (4.2) and changing the variables as $t \rightarrow \lambda t$, $t' \rightarrow \lambda t'$, $r \rightarrow \gamma r$ and $r' \rightarrow \gamma r'$, we find (4.2) to be consistent with the untransformed equation with T replaced by T^λ only if

$$T^\lambda = (\lambda/\gamma^2) T \quad (4.4)$$

$$\phi_G^\lambda(r) = (\gamma/\lambda)^2 \phi_G(r/\gamma) \quad (4.5)$$

The boundary condition (3.19) is satisfied on the interfaces of the transformed domain structure. When (4.3) is used, the expressions (3.21) and (3.22) for the transformed state can now be found to be compatible with (4.3) if we require

$$Z^\lambda(T) = Z(T^\lambda)/\gamma \quad (4.6)$$

Here we have noted that

$$\int_{\Sigma_T} da \dots$$

becomes after change of variables $da \rightarrow \gamma^2 da$

$$\int_{\Sigma_T} da \dots \rightarrow \left(\frac{\lambda}{\gamma^3} \right) \gamma^2 \int_{\Sigma_T} da = \frac{\lambda}{\gamma} \int_{\Sigma_T} da \quad (4.7)$$

where the factor λ/γ^3 takes care of the change of the total number of domains by the transformation. However, we have under the same change of variables

$$\int_{\Sigma^\lambda(r)} da \dots \rightarrow \gamma^2 \int_{\Sigma(r)} da \quad (4.8)$$

since here only a single domain is involved.

The result (4.6) permits us to derive the scaling relation for $H_G\{\bar{\psi}\}$. Thus using (3.25)

$$\begin{aligned} H_G^\lambda(\{\bar{\psi}^\lambda\}, T) &= -nT \ln Z^\lambda(T) = -nT \ln Z(T^\lambda) + nT \ln \gamma \\ &= \frac{T}{T^\lambda} H_G(\{\bar{\psi}\}, T^\lambda) + nT \ln \gamma \end{aligned}$$

That is, upon introduction of the free energy per chain, $h_G = H_G/n$

$$h_G^\lambda(\{\bar{\psi}^\lambda\}, T) = \frac{\gamma^2}{\lambda} h_G\left(\{\bar{\psi}\}, \frac{\lambda}{\gamma^2} T\right) + T \ln \gamma \quad (4.9)$$

So far our argument has been quite general in SSR. We now assume that, in block copolymers consisting of very long chains, domain sizes are much greater than the gyration radius of a chain R_g , which transforms as $R_g^\lambda = \lambda^{1/2} R_g$. We now imagine that we construct a state of very

large domain size with very long chains by the transformation with very large λ and γ . Our assumption then implies that $\gamma \gg \lambda^{1/2}$. Equation 4.9 then implies that we are mapping the state with a very large domain size and very long chains into another state with a very low temperature. For the latter state (3.9) indicates that the chain propagates along the "classical path" that minimizes the "action" in (3.9). $\phi_G(\mathbf{r})$ is then determined by (3.22) where the classical approximation can be used to obtain the \bar{Q} 's.¹⁰ This then suggests that $T \ln Z(T)$ and hence $h_G(T)$ becomes asymptotically independent of T as T approaches zero. If we identify $\{\bar{\psi}\}$ in (4.9) as the state $\{\psi\}$ under consideration and note that λ and γ are then proportional to N and the domain size D , (4.9) suggests the following form for h_G where T in the argument is now suppressed.

$$h_G\{\bar{\psi}\} = \frac{D^2}{N} h_G^*\{\psi^*\} + T \ln(D/z_J) \quad (4.10)$$

where $h_G^*\{\psi^*\}$ is the reference free energy per chain of unit length in a reference domain state $\{\psi^*\}$ with the unit domain size. The first term of (4.10) is the free energy of chain stretching and the second term arises from the loss of entropy due to confinements of chain junction points in narrow interfacial regions of the width z_J .⁴ Equation 4.10 must be supplemented with interfacial energy per chain

$$h_s\{\bar{\psi}\} = \sigma A_1 \quad (4.11)$$

where A_1 is the interfacial area per chain. Since A_1 is proportional to N/D , we can write

$$h_s\{\bar{\psi}\} = \frac{N}{D} h_s^*\{\psi^*\} \quad (4.12)$$

$h_s^*\{\psi^*\}$ and also $h_G^*\{\psi^*\}$ are the numbers independent of N and are determined by the domain morphology expressed by $\{\psi^*\}$.

Once we assume a morphology ψ^* , the domain size can then be determined by minimizing the total free energy per chain:

$$\frac{\partial}{\partial D} [h_s\{\bar{\psi}\} + h_G\{\bar{\psi}\}] = 0 \quad (4.13)$$

It turns out that, for sufficiently large N , the second term in (4.10) gives only a small correction. Thus, up to the first order in this correction, which is linear in T , we have for the optimum value of D

$$D = D^* \equiv \{h_s^*/(2h_G^*)\}^{1/3} N^{2/3} - \frac{T}{6} (h_G^*)^{1/3} (h_s^*)^{-4/3} N^{1/3} \quad (4.14)$$

Substituting this result into h_G and h_s , we obtain for the total free energy per chain h_T up to first order in T

$$h_T = 3(2^{2/3})(h_s^*)^{2/3}(h_G^*)^{1/3} N^{1/3} + \frac{T}{3} \ln(h_s^*/h_G^*) + \frac{T}{3} \ln(N^2/2z_J^3) \quad (4.15)$$

This result can then be used to find the morphology $\{\psi^*\}$, which minimizes the total free energy and hence represents the equilibrium state. Note that the final result is independent of particular definitions of D for different morphologies since the arbitrariness in these choices is absorbed into the definitions of h_s^* and h_G^* and does not affect values of the free energy (4.15). A convenient choice of D would be to take it as the periodicity of mesophase structures.

Here we point out that the problem of determination of morphology in SSR by (4.15) is now purely geometrical

including a small correction of order $TN^{-1/3}$ whose coefficient is again determined by the geometry of the domain structure.

5. Lamellar Phase

Here we illustrate our theory of block copolymer morphology in SSR assuming the lamellar structure. Since we need to consider spatial variations only in the direction (the x direction) perpendicular to the lamellae, we examine a cylindrical portion of the system whose axis is along the x direction. The length of the cylinder is taken to be D , the periodicity, and the cross section to be $A_1 = N/(D\rho_0)$ so that the cylinder has the volume $V_1 = N/\rho_0$ containing a single chain on the average. We can then treat the system as though it is one-dimensional. Let us choose the origin $x = 0$ on one of the interfaces, and the cylinder extends from $x = -D_B$ to D_A with $D_A \equiv fD$ and $D_B \equiv (1-f)D$, so that the cylinder is bounded by other interfaces on both sides. We then find from (3.21) by noting that $A_1/V_1 = D^{-1}$ and by symmetry

$$Z = 2 \frac{z_J}{D} \bar{q}_A \bar{q}_B \quad (5.1)$$

where

$$\bar{q}_A \equiv \int_0^{D_A} \bar{Q}_{J_0^A}(0, x) dx \quad (5.2a)$$

$$\bar{q}_B \equiv \int_{-D_B}^0 \bar{Q}_{N_J^B}(x, 0) dx \quad (5.2b)$$

Here the \bar{Q} 's are for a one-dimensional system satisfying the one-dimensional version of (3.17)–(3.19) written out explicitly only for $K = A$ as

$$\frac{\partial}{\partial t} \bar{Q}_{tt'}^A(xx'; \{\phi_G\}) = \left[\frac{T}{2} \frac{\partial^2}{\partial x^2} + T^{-1} f_A \phi_G(x) \right] \bar{Q}_{tt'}^A(xx'; \{\phi_G\})$$

$$N_A \geq t \geq t' \geq 0 \quad (5.3)$$

$$\bar{Q}_{tt'}^A(xx'; \{\phi_G\}) = \delta(x-x') \quad (5.4)$$

$$\frac{\partial}{\partial x} \bar{Q}_{tt'}^A(xx'; \{\phi_G\}) = \frac{\partial}{\partial x} \bar{Q}_{tt'}^A(x'x; \{\phi_G\}) = 0$$

for $x = 0$ and D_A (5.5)

Equation 3.22a also reduces by use of (5.3) and by symmetry to

$$\frac{D}{2N\bar{q}_A} \int_0^{N_A} dt \int_0^{D_A} dx' [\bar{Q}_{N_A t}^A(0, x'; \{\phi_G\}) + \bar{Q}_{N_A t}^A(D_A, x'; \{\phi_G\})] \bar{Q}_{t_0}^A(x, x'; \{\phi_G\}) = 1$$

for $0 < x < D_A$ (5.6a)

Similarly we find

$$\frac{D}{2N\bar{q}_B} \int_{N_A}^N dt \int_{-D_B}^0 dx' [\bar{Q}_{N t}^B(-D_B, x'; \{\phi_G\}) + \bar{Q}_{N t}^B(0, x'; \{\phi_G\})] \bar{Q}_{t_0}^B(x, x'; \{\phi_G\}) = 1$$

for $-D_B < x < 0$ (5.6b)

Since in SSR an A-type chain is completely confined inside one A-rich domain, $\bar{Q}_{tt'}^A$ depends only on ϕ_G inside the single A-rich domain. Thus the above result indicates that, for the lamellar morphology, the problem of determining the \bar{Q} 's and hence the free energy contribution in each domain is completely separable, i.e., is independent of states of other domains. This simplifying feature, unfortunately, is limited only to the lamellar morphology where the number of junction points per unit interfacial area (the junction point density) is fixed at $\rho_0 D/2N$. For other morphologies, different parts of interfaces are not

always equivalent in the sense that the domain configurations surrounding them cannot be superimposed by means of some translations, rotations, and reflections. Therefore, the junction point density, in general, differs from one point on the interface to another, which is affected by states of the two domains on both sides of the interface, and hence the independence of different domains is lost.

The free energy per block copolymer chain in the lamellar phase is now written as

$$h = 2\sigma N/D\rho_0 - T \ln \bar{q}_A - T \ln \bar{q}_B + T \ln D/2z_j \quad (5.7)$$

We see that this expression coincides with the one obtained by Helfand and Wasserman⁴ apart from a term that does not contain D .

6. Classical Limit and the Semenov Theory

In the scaling limit where D greatly exceeds the chain gyration radius R_g , we can use the classical path approximation as we have noted in section 4. We write down the expression for $\bar{Q}_{tt'}^A(xx';\{\phi_G\})$ for an A-rich lamellar domain in this limit¹¹

$$\bar{Q}_{tt'}^A(xx';\{\phi_G\}) = \{2^{1/2}\pi T\}^{-1/2} \{ [E - f_A\phi_G(x)]^{1/2} [E - f_A\phi_G(x')]^{1/2} \int_x^{x'} dy [E - f_A\phi_G(y)]^{-3/2} \}^{1/2} \times \exp(T^{-1}) \left\{ \int_t^{t'} ds \left[-\frac{1}{2}\dot{c}(s)^2 + f_A\phi_G(c(s)) \right] \right\} \quad (6.1)$$

where

$$E = \frac{1}{2}\dot{c}(s)^2 + f_A\phi_G(c(s)) = E(xx',tt') \quad (6.2)$$

is the "total energy" of the classical path, which is independent of s . This classical path is given by solving the equation

$$\dot{c}(s) = -f_A\phi_G'(c(s)) \quad (6.3)$$

under the conditions

$$c(t') = x' \text{ and } c(t) = x \quad (6.4)$$

where the prime on ϕ_G denotes differentiation. The function $\phi_G(x)$ is determined by (5.6a) where (5.5) may not be satisfied in the classical limit. See below.

On the other hand, recently Semenov⁵ proposed a theory of block copolymers that is designed to describe the classical limit. This theory will now be discussed in the context of our theory (see also ref 12). Here, since two A-block chains with junction points on the two interfaces bounding the A domain under consideration do not overlap, we can limit our consideration to a single A-block chain with the junction point at $x = 0$ and the free end point x_0 between x and $R \equiv (1/2)D_A$. Upon introduction of the end-point probability distribution $g(x_0)$, the elastic energy of the A-block chain h_A is

$$h_A = \frac{1}{2} \int_0^R dx_0 g(x_0) \int_0^{x_0} dc v(c) \quad (6.5)$$

where $v(c)$ is the size of the "velocity" $\dot{c}(s)$ at $c(s) = c$ of the classical path $c(s)$ starting at $c(0) = x_0$ with zero speed $\dot{c}(0) = 0$ corresponding to the free end and ending at $c(N_A) = 0$. Since the path starting at different x_0 must reach the point $x = 0$ during the time interval N_A , which is independent of x_0 , the motion must be that of a harmonic oscillator¹² such that

$$f_A\phi_G'(x) = \omega^2 x \quad (6.6)$$

where ω is a fixed angular frequency given by

$$\omega = \pi/2N_A \quad (6.7)$$

since N_A is one-fourth of the oscillation period $2\pi/\omega$. We thus find

$$c(t) = x_0 \cos \omega t \quad (6.8)$$

Hence we immediately obtain

$$v(c) = (\pi/2N_A)(x_0^2 - c^2)^{1/2} \quad (6.9)$$

Using the normalization condition

$$\int_0^R dx_0 g(x_0) = 1 \quad (6.10)$$

and the following condition of the uniform monomer density at x , which is contributed from chains whose free ends are between x and R

$$\int_x^R dx_0 \frac{g(x_0)}{v(x;x_0)} = \frac{N_A}{R} = \frac{2N_A}{D_A} \quad (6.11)$$

where $v(x;x_0)$ is the velocity at x of a chain whose end point is at x_0 . From (6.9)–(6.11), we find

$$g(x_0) = \frac{1}{R} \frac{x_0/R}{[1 - (x_0/R)^2]^{1/2}} \quad (6.12)$$

Substitution of (6.9) and (6.12) into (6.5) yields the following result for h_A expressed in terms of D_A :

$$h_A = \frac{\pi^2 D_A^2}{96 N_A} \quad (6.13)$$

Now, if the potential (6.6) were indeed the correct one in the classical limit, we should be permitted to use this potential to obtain the classical chain propagator (6.1). After some algebra we find with ω given by (6.7)

$$\bar{Q}_{tt'}^A(xx';\{\phi_G\}) = \left[\frac{2\pi T}{\omega} \sin \omega(t-t') \right]^{-1/2} \times \exp \left\{ -\frac{\omega}{2T \sin \omega(t-t')} [(x^2 + x'^2) \cos \omega(t-t') - 2xx'] \right\} \quad (6.14)$$

This propagator, however, appears to violate the condition (5.5). Indeed, the following expression obtained from (6.14)

$$\frac{\partial}{\partial x} \bar{Q}_{tt'}^A(xx';\{\phi_G\}) = -\frac{\omega}{T \sin \omega(t-t')} [x \cos \omega(t-t') - x'] \bar{Q}_{tt'}^A(xx';\{\phi_G\})$$

does not vanish at the interface $x = 0$ as is required by (5.5). This conflict arises from the fact that harmonic potential (6.6) is insufficient to prevent chains from leaking through the interface. In order to avoid this difficulty, a hard wall at the interface ($x = 0$) must be added to the harmonic potential. As will be described in the next section, we can verify by numerical analysis of the coupled equations (5.3)–(5.5) that the exact self-consistent potential, $\phi(x)$, actually has a δ -function-type steep wall at the interface. Such a hard wall, however, affects only segments near the interface because, in the classical limit, the fluctuation in the chain conformation in the x direction is quite small and the effects of the reflection of the path by the hard wall are negligible.

Next we examine the left-hand side of (5.6a) where the second term in the square bracket should drop in the classical limit and the integral over x' is limited to the interval $(x, D_A/2)$. Hence we have by suppressing $\{\phi_G\}$ in

the arguments

$$\frac{D}{2N\bar{q}_A} \int_0^{N_A} dt \int_x^{D_A/2} dx_0 \bar{Q}_{N_A t}^A(0x) \bar{Q}_{t_0}^A(xx_0) \quad (6.15)$$

This expression in the classical limit is analyzed in Appendix B with the following result:

$$\begin{aligned} (6.15) &= \frac{1}{\pi} \ln \frac{1 + [1 - (x/R)^2]^{1/2}}{1 - [1 - (x/R)^2]^{1/2}} \\ &\simeq \frac{2}{\pi} \ln \frac{R}{x} \quad x \ll R \\ &\simeq \frac{2}{\pi} \left[2 \left(1 - \frac{x}{R} \right) \right]^{1/2} \quad R - x \ll R \end{aligned} \quad (6.16)$$

This is far from a constant, logarithmically diverging at the origin and vanishing at $x = R$. This result is consistent with the fact that the chain-end distribution, which is proportional to $\bar{Q}_{N_A 0}^A(0x)$, is a constant (see (B.3)) in contrast to the Semenov distribution (6.12). One can also discuss the free energy contribution \bar{h}_A of an A-block chain, which corresponds to (6.13). Here we must start from (3.20) since (3.24) is not true for

$$f_A \phi_G(x) = \frac{1}{2} \omega^2 x^2 \quad (6.17)$$

Using (5.1) where Z is replaced by \bar{q}_A , the contribution of a single A-block chain, given by (B.6), and performing the integral in the second term of (3.20) over the volume $(N/D\rho_0) \times D_A$ occupied by a single A-block chain, we find

$$\begin{aligned} \bar{h}_A &= -T \ln \bar{q}_A + \frac{N}{D\rho_0} \int_0^{D_A} dx \rho_0 f_A \phi_G \\ &= -T \ln \left[\frac{D_A}{4(N_A T)^{1/2}} \right] + \frac{\pi^2 D_A^2}{96 N_A} \end{aligned} \quad (6.18)$$

The first term is the entropy contribution arising from the uniform end-point distribution inside half of the A-rich domain. The second term is precisely the Semenov result, which is expected since we have used Semenov's harmonic potential for $f_A \phi_G$. The main difficulty, however, is the nonuniformity of $\bar{\psi}(x)$ inside each domain as is evidenced by (6.16).

The difference between our theory and the Semenov theory seems to arise from the fundamentally different manner in which the end-point distribution is treated. Semenov averages the free energy over the end-point distribution, which is analogous to the way the quenched disorder is treated in random systems.¹³ On the other hand, we effectively average the partition function, which corresponds to annealing the disorder¹³ and is more appropriate in dealing with true thermal equilibrium.

Very recently, a way out of this dilemma was suggested by Milner, Wang, and Witten.¹⁴ They argue that the harmonic potential (6.6) is not precise enough to obtain the correct end-point distribution, and (6.6) must be supplemented by an additional term. This term is negligibly small for large N_A except in the immediate vicinity of $x = 0$ and $x = R$ where it becomes singular. The correction to \bar{h}_A (6.18), arising from this term turns out to be $O(T)$ and is negligible in the classical limit. In Appendix C we examine the classical limit ($T \rightarrow 0$) of our theory without assuming the harmonic potential from the outset.

We may thus conclude that, despite different formal appearances, the Semenov theory and the field theoretical treatment lead to the same result in the classical strong segregation limit.

7. Numerical Computation

Now, it is important to test the results obtained in sections 4–6 by numerical computation. We restrict ourselves only to the lamellar case for which it is rather easier to perform computation. Thus we have to solve (5.3) under the conditions (5.4) and (5.5) to obtain the exact propagator $\bar{Q}_{tt'}^A(xx';\{\phi_B\})$. Such a computation was performed previously by Helfand and Wasserman.^{4b} Helfand and Wasserman calculated the propagator by decomposing it into the normal modes to reduce the degrees of freedom of the system. Here, however, we solve the partial differential equation (5.3) directly, and thus our method is rather similar to that used by Viovy et al.¹⁵ Contrary to our condition (5.5), however, Viovy et al. used the boundary condition $\bar{Q}_{tt'}(0x';\{\phi_G\}) = 0$, whose physical origin is not clear to us. In the following, our numerical procedure is summarized.

We solve (5.3), with $T = 1.0$ and $f = 1/2$ for simplicity, using the implicit difference scheme, which is more stable than the naive explicit scheme. To obtain the correct functional form of $\phi_G(x)$, we carry out an iterative refinement of $\phi_G(x)$ starting from an appropriately chosen first trial function denoted as $\phi^{(0)}(x)$. If the i th trial $\phi^{(i)}(x)$ is given, we solve (5.3) with this trial $\phi^{(i)}(x)$ and calculate the propagator $\bar{Q}_{tt'}(xx';\{\phi^{(i)}\})$. The reduced monomer density profile $\hat{\rho}^{(i)}(x)$ is evaluated by using (5.6a) as

$$\frac{D}{2N\bar{q}_A} \int_0^{N_A} dt \int_0^{D_A} dx' [\bar{Q}_{N_A t}^A(0x';\{\phi^{(i)}\}) + \bar{Q}_{N_A t}^A(D_A x';\{\phi^{(i)}\}) \bar{Q}_{t_0}^A(xx';\{\phi^{(i)}\})] = \hat{\rho}^{(i)}(x) \quad (7.1)$$

where the right-hand side is not necessarily unity unless the trial $\phi^{(i)}$ is the correct one. As the density profile is required to be unity throughout the entire system (see (5.6a)), we refine the field $\phi^{(i)}(x)$ so that the $\hat{\rho}(x)$ approaches everywhere to unity. Here we employ the local tangent approximation given as

$$\phi^{(i+1)}(x) = \phi^{(i)}(x) + \alpha [\hat{\rho}^{(i)}(x) - 1] \quad (7.2)$$

where α is some positive constant coefficient.¹⁵ The iteration is continued until the ratio of the difference between $\hat{\rho}(x)$ and its aimed value 1.0 becomes everywhere less than ϵ , where we select ϵ to be 10^{-5} . For the first trial $\phi^{(0)}(x)$, we take $\phi^{(0)}(x) \equiv 0$. By integrating (7.1) with respect to x over an A domain, we find

$$\int_0^{D_A} dx [\hat{\rho}^{(i)}(x) - 1] = 0$$

It is, therefore, obvious that the iterative scheme (7.2) preserves the quantity

$$\int_0^{N_A} \phi^{(i)}(x) dx$$

which is identically zero because of our choice of the first trial $\phi^{(0)}(x)$ to be identically zero.

We found that the computed potential $\phi_G(x)$ has a δ -function-like singularity at the interface, which was also reported by Helfand and Wassermann,^{4b} and due to such a singularity, the convergence of the iterative scheme (7.2) becomes poor especially in the nonclassical region. The accuracy of the results was checked by changing the numbers of mesh points in t and x , and we confirmed that for sufficiently large numbers of mesh points the difference between the results obtained with different sets of mesh numbers is quite small, say, within a few percent.

In the following, we present our numerical results and compare them with those of Helfand and Wasserman^{4b} and of Semenov.⁵ We take up the partition function (3.12).

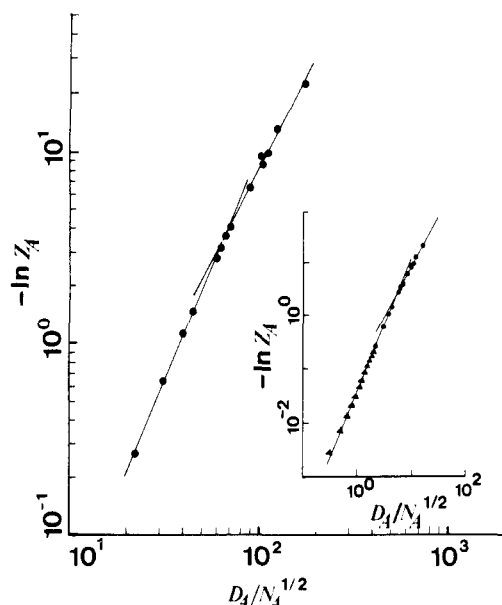


Figure 2. Scaling behavior of the logarithm of the partition function of an A domain, Z_A . Two regions can be observed with a crossover around $D_A/N_A^{1/2} \simeq 7.0$. The slopes of the straight lines (determined by the least-squares fit) are 2.41 ± 0.03 and 1.96 ± 0.05 , respectively. The inset explains the relation between our data (circles) and those of Helfand and Wasserman (triangles).

Helfand and Wasserman computed the partition function of a chain in an A domain, Z_A , which is defined as

$$Z_A \equiv \frac{1}{D_A} \int_0^{D_A} dx \int_0^{D_A} dx' Q_{N_A 0}^A(x, x')$$

We can confirm that the relation $\tilde{h}_G \equiv H_G\{\tilde{\psi}\}/n = -T \ln [Z_1\{\phi_G\}/Z_1\{0\}]$ holds from (3.12) and (3.25), and for a chain in an A domain it reduces to $h_A = -T \ln Z_A\{\phi_G\} + h_A'$, where h_A' arises from the normalizing factor in (3.12) and has a weak (logarithmic) dependence on D_A . Thus we can identify h_A with $-\ln Z_A\{\phi_A\}$ for the $T = 1.0$ case. Helfand and Wasserman obtained the scaling behavior

$$-\ln Z_A = 0.0357(D_A/N_A^{1/2})^{2.5} \quad (7.3a)$$

by fitting the numerical data.¹⁶ This result conflicts with our result (4.10), which is given by

$$-\ln Z_A \sim (D_A/N_A^{1/2})^2 \quad (7.3b)$$

apart from a small logarithmic correction. In Figure 2 we show the dependence of Z_A on $D_A/N_A^{1/2}$ obtained by our computation. In this figure, as we go from the left to the right, we approach the classical limit, which was discussed in section 6. Clearly we see a crossover from the region $-\ln Z_A \propto (D_A/N_A^{1/2})^{2.4}$ (region I) to the region $-\ln Z_A \propto (D_A/N_A^{1/2})^2$ (region II) around $D_A/N_A^{1/2} \simeq 7.0$. To make a quantitative comparison with the result of Helfand and Wasserman and with the classical theory, we draw the two straight lines in the figure by the least-squares fit, leading to the following scaling laws:

$$-\ln Z_A = (0.039 \pm 0.002)(D_A/N_A^{1/2})^{2.41 \pm 0.03} \quad (\text{region I}) \quad (7.4a)$$

$$-\ln Z_A = (0.090 \pm 0.010)(D_A/N_A^{1/2})^{1.96 \pm 0.05} \quad (\text{region II}) \quad (7.4b)$$

In region I, the prefactor of (7.4a) is 0.039 ± 0.002 and this coincides with that obtained by Helfand and Wasserman, (7.3a). On the other hand, in region II, where the system is near the classical limit, the scaling law, (7.4b), can be compared with that of Semenov, (6.13). The pre-

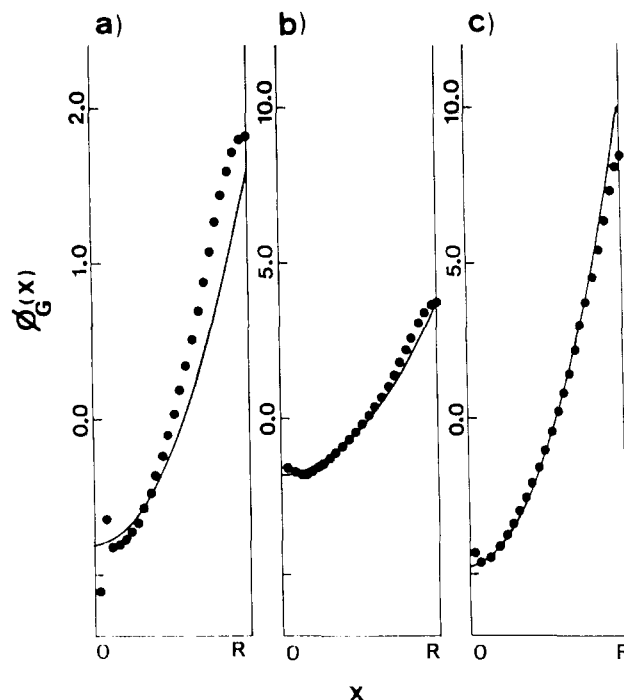


Figure 3. Self-consistent potential, $\phi_G(x)$, in an A domain calculated and shown by solid circles for each of the parameter set: (a) $D_A = 10.0$, (b) $D_A = 15.0$, and (c) $D_A = 25.0$, all with $N_A = 5.0$ and $f = 1/2$. In the figure, only half of the A domain is shown because of the symmetry with respect to the midpoint plane of the domain. The solid lines represent Semenov's harmonic potentials.

factor of (7.4b) is 0.090 ± 0.010 , which is consistent with Semenov's value $\pi^2/96 = 0.103$ given in (6.13). It is, therefore, concluded that Helfand and Wasserman's result pertains to the former regime (region I), which we can regard as the transient one, and the scaling argument in section 4 gives the correct asymptotic behavior.

Next we turn to the potential function and the end density distribution. In Figure 3 we represent the computed self-consistent potential, $\phi_G(x)$, by solid circles and Semenov's parabolic potential function (6.17) by solid curves, where an irrelevant constant term is added so as to fit the curves to those of our computer results. The parameters are $N_A = 5.0$, $f = 1/2$, and (a) $D_A = 10.0$ (in region I), (b) $D_A = 15.0$ (near the crossover point), and (c) $D_A = 25.0$ (in region II), respectively. Here the δ peak at $x = 0$ is too large to be shown in these figures. As is expected, the functional form of the potential $\phi_G(x)$ approaches more and more to the harmonic one, except for the singularity at the domain wall and the small region near the midpoint of the domain. Recently, Milner et al. discussed the potential function of a grafted polymer surface in the classical limit.¹⁴ They considered the potential of the form

$$\phi(x) = \frac{1}{2}\omega^2 x^2 + V(x) \quad (7.5)$$

where $V(x)$ is a weak perturbation. Using the unperturbed classical path, they found that the perturbation $V(x)$, which gives the desired end density (6.12), has the following form:

$$V(x) = \frac{1}{N} \left[\ln x + \left(\frac{x}{R-x} \right)^{1/2} \arctan \left(\frac{x}{R-x} \right)^{1/2} \right] \quad (7.6)$$

The perturbation $V(x)$ diverges logarithmically at $x = 0$ and as $(R-x)^{-1/2}$ at $x = R$. As is shown in Figure 3 we can observe a singularity near the interface in our numerical calculation, which should be identified with first term in

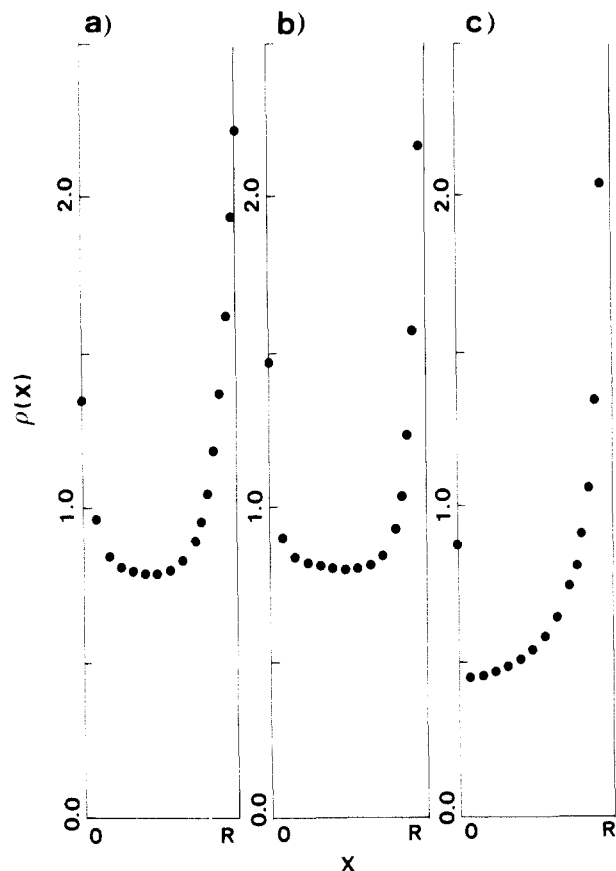


Figure 4. Monomer density distribution computed by the field theoretical calculation using the perturbed potential (7.5) and (7.6) shown for the three cases in Figure 3.

(7.6). On the other hand, we cannot observe the divergence at $x = R$ by the numerical calculation, which is a result of the interpenetration between the block chains coming from the opposing interfaces in a domain.¹⁷ As such an interpenetration is not taken into account in the classical end density, (6.12), the monomer density of chains grafted onto one of the interfaces must be sharply cut off at the midpoint of the domain, giving rise to the divergence at $x = R$ in (7.6). As is seen from Figure 3, we can avoid such divergence by taking account of the interpenetration. To test the validity of the above-mentioned perturbation theory of Milner et al. in our lamellar case, we obtained the monomer density profile by using the potential (7.5) supplemented with (7.6) by using our field theoretical calculation. The results are shown in Figure 4. If (7.6) were correct, the monomer density would be expected to be uniform in the classical limit. The uniformity near the domain boundary holds better as the system approaches the classical limit, but the monomer density is far from uniform at the midpoint of the domain, which may signify breakdown of the perturbation (7.6) at $x = R$ because of the interpenetration.

The extent of the interpenetration can be shown directly by computing the end-point density of the chains, and the results are displayed in Figure 5, where the parameters are the same as those in parts a–c of Figure 3. In these figures, circles represent $g(x)$, the end-point density of all the chains that are inside the domain, defined as

$$g(x) \equiv (\bar{Q}_{j0}^A(0, x) + \bar{Q}_{j0}^A(D_A, x)) / \int_0^{D_A} \bar{Q}_{j0}^A(0, x) dx \quad (7.7a)$$

and the triangles represent $g'(x)$, the end density of the chains that are grafted onto the left-side interface at $x =$

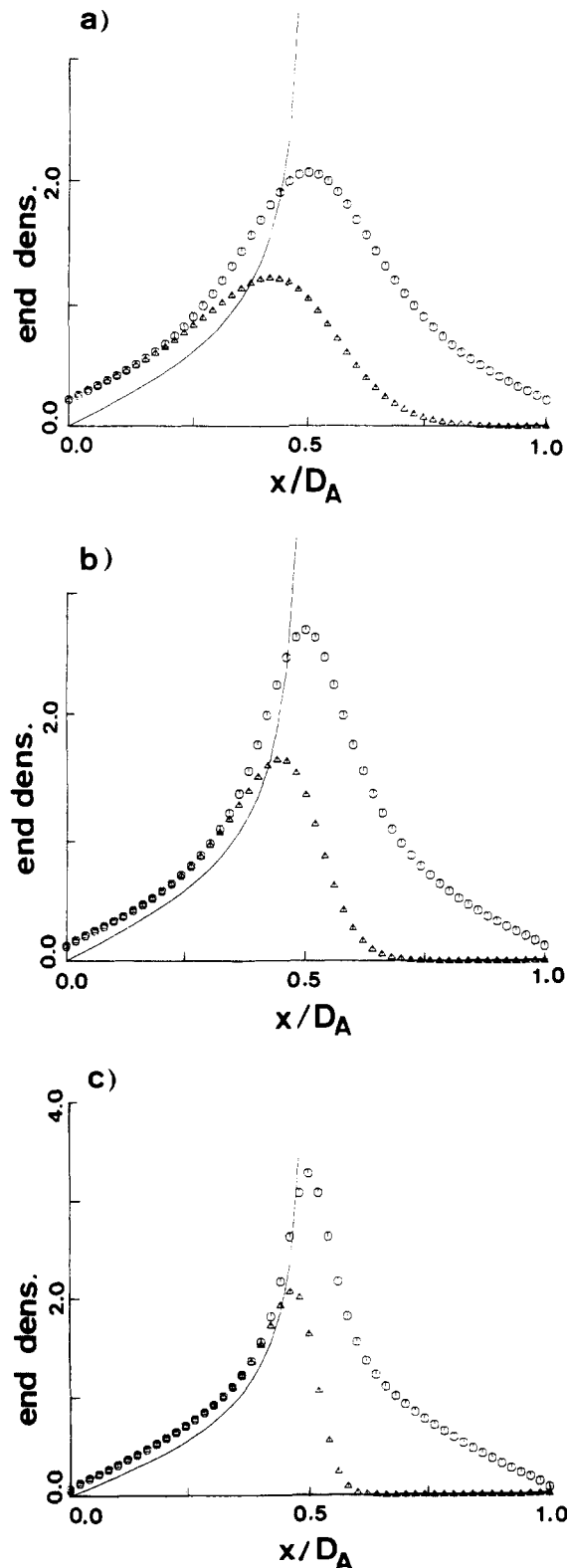


Figure 5. End-point density distributions for the cases (a)–(c) of figure 3. The circles, the triangles, and the solid curve show $g(x)$ (7.7a), $g'(x)$ (eq. (7.7b)) and Semenov's theoretical result (eq. (6.12)), respectively.

0, given by

$$g'(x) \equiv \bar{Q}_{j0}^A(0, x) / \int_0^{D_A} \bar{Q}_{j0}^A(0, x) dx \quad (7.7b)$$

The theoretical end-point density in the classical limit (6.12) obtained by Semenov is also shown by the solid curves. In the classical limit, the chains grafted onto the left-side interface at $x = 0$ are completely separated at the midpoint of the domain, $x = D_A/2$, from those grafted onto

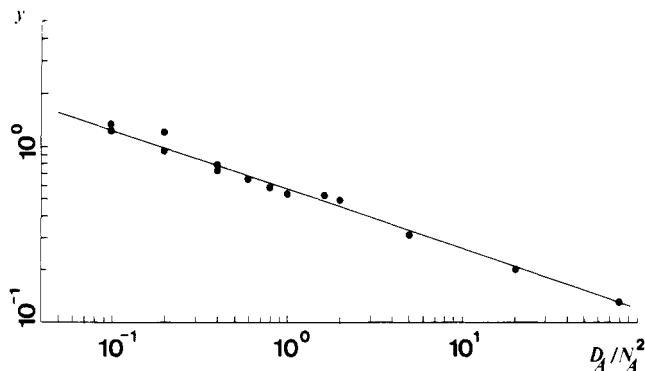


Figure 6. Dependence of y , the extent of the interpenetration, on the quantity (D_A/N_A^2) . The straight line is a least-squares fit, which shows the relation $y \sim (D_A/N_A^2)^{-1/3}$ obtained by Witten et al.¹⁷

the right-side interface at $x = D_A$, and, therefore, the end density, $\rho'(x)$, in Figure 5 decays rapidly beyond the midpoint. It can be seen, however, that there are some chains that start in the right half of the domain and end at the left-side interface (the tail of ρ' beyond the midpoint), which is due to the thermal fluctuations in the conformation of chains. Witten et al.¹⁷ showed theoretically that the extent of the interpenetration length, denoted as y , is proportional to $(D_A/N_A^2)^{-1/3}$. We evaluated this quantity y from our simulation data, and the results are shown in Figure 6. Here we defined y as the distance between the midpoint of the domain and the point where $g'(x)$ takes the half value of its maximum. The straight line in the figure is the least-squares fit of the data, which is represented by

$$y = (0.57 \pm 0.01)(D_A/N_A^2)^{-0.337 \pm 0.01} \quad (7.8)$$

This clearly verifies the prediction of Witten et al.¹⁷

It is obvious from Figures 3, 5, and 6 that the classical path approximation in Semenov's theory becomes worse when we enter the nonclassical regime (for example, parts a and b of Figure 5). In view of our findings it would be very much worthwhile to investigate the approach to the classical limit more systematically employing, e.g., the WKB-like method.

8. Concluding Remarks

The field theoretical formulation of block copolymer melts was made useful for the investigation of the equilibrium morphology of microphase-separated states in the strong segregation regime by introducing the following assumptions:

- (1) The monomer concentration profile characteristic of the strong segregation limit is assumed where the concentration variable inside each domain is uniform.
- (2) The free energy functional, $H\{\psi\}$, can be split into two parts involving short-range and long-range effective interactions between the local concentration variables.
- (3) The part involving short-range interactions reduces to the domain wall energy apart from an unimportant constant contribution.
- (4) The part involving long-range interactions can be obtained by Gaussian chain statistics.

The earlier result of Helfand and co-workers⁴ and that of Semenov⁵ for the case of lamellar phase basically follow from our theory.

Developing a computational scheme for more complicated morphologies than the lamellar phase remains a challenging future problem. On the other hand, a computationally simpler model such as the one suggested in

OK still has some attractive features although justification of such a model is a formidable task.

Finally we briefly mention an analogy between our field theory of the block copolymer systems and the density functional theory (DFT) of the quantum electronic systems.^{18,19} In the DFT, the one-body wave function of the i th quantum state, $\psi_i(\mathbf{r})$, is determined from the so-called "Kohn-Sham equation":

$$\left[-\frac{1}{2}\nabla^2 + V_{\text{eff}}(\mathbf{r}) \right] \psi_i(\mathbf{r}) = \epsilon_i(\mathbf{r}) \psi_i(\mathbf{r}) \quad (8.1)$$

The effective potential, $V_{\text{eff}}(\mathbf{r})$ includes the many-body correlation effects and is given by

$$V_{\text{eff}}(\mathbf{r}) = V(\mathbf{r}) + \int \frac{n(\mathbf{r}')}{|\mathbf{r}-\mathbf{r}'|} d\mathbf{r}' + \frac{\delta E_{\text{XC}}[n(\mathbf{r})]}{\delta n(\mathbf{r})} \quad (8.2)$$

where $V(\mathbf{r})$ is the potential by the ion cores, $E_{\text{XC}}[n(\mathbf{r})]$ accounts for the exchange and the correlation between the electrons, and

$$n(\mathbf{r}) = \sum_{i=1}^N |\psi_i(\mathbf{r})|^2 \quad (8.3)$$

is the density distribution of the electrons. Assuming the functional form of $E_{\text{XC}}[n(\mathbf{r})]$ and solving the coupled equations (8.1)–(8.3) self-consistently, we can obtain the correct density distribution $n(\mathbf{r})$. We notice that (8.1) is similar to (3.11), where the functions $\psi_i(\mathbf{r})$ and $V_{\text{eff}}(\mathbf{r})$ corresponds to $Q_{it}(\mathbf{r}, \mathbf{r}')$ and $\phi(\mathbf{r})$, respectively. The main difference in the methodology is as follows: In the DFT the wave function $\psi_i(\mathbf{r})$ is obtained by assuming the effective potential V_{eff} , while in our field theory of block copolymers the effective potential $\phi(\mathbf{r})$ is determined by assuming the distribution of the monomer density. Except for such a difference, these two methods have some similarities both in the formulation and in the numerical techniques. We may be able to learn a lot from the DFT if we take advantage of such an analogy.

Acknowledgment. K.K. acknowledges a very enlightening conversation with Professor T. A. Witten on the classical limit of the block copolymer theory. T.K. thanks Dr. W. Zimmermann for useful discussions on the computational scheme. It is a pleasure to thank an anonymous referee, who carefully read the original version of the manuscript and made pertinent comments, which were of enormous help in preparing the final version. The work was partially supported by the Scientific Research Fund of the Ministry of Education, Science and Culture of Japan.

Appendix A

Here we shall discuss the excluded-volume potential between chain segments in polymer melts that may be stretched. We make the problem somewhat more general by considering a test chain immersed in the matrix consisting of n polymer chains of the same kind which may differ from the test chain. In this section a suffix zero is attached to all the quantities referring to the test chain. The interaction Hamiltonian of the test chain and the matrix is taken to be of the form

$$\begin{aligned} H'(\mathbf{c}_0, \mathbf{c}) &= \sum_{i=1}^n \int_0^{N_0} dt_0 \int_0^N dt v_{it_0}(\mathbf{c}_0(t_0) - \mathbf{c}_i(t)) \\ &= - \int_0^N dt \int d\mathbf{r} \hat{\phi}(t, \mathbf{r}; \mathbf{c}_0) \hat{\rho}(t, \mathbf{r}) \end{aligned} \quad (A.1)$$

where

$$\hat{\rho}(t, \mathbf{r}) \equiv \sum_{i=1}^n \delta(\mathbf{r} - \mathbf{c}_i(t)) \quad (\text{A.2})$$

$$\hat{\phi}(t, \mathbf{r}; \mathbf{c}_0) \equiv - \int_0^{N_0} dt_0 v_{t_0}(\mathbf{c}_0(t_0) - \mathbf{r}) \quad (\text{A.3})$$

The partition function for the entire system is, with T chosen to be unit in this section for simplicity

$$Z_{\text{total}} = \int d\{\mathbf{c}_0\} \exp[-\hat{H}_0(\mathbf{c}_0)] Z_M\{\hat{\phi}(\cdot, \cdot; \mathbf{c}_0)\}$$

where $\hat{H}_0(\mathbf{c}_0)$ is the Hamiltonian of an isolated test chain and $Z_M\{\phi\}$ is defined for an arbitrary function $\phi(t, \mathbf{r})$ of \mathbf{r} and t by

$$Z_M\{\phi\} \equiv \int d\{\mathbf{c}\} \exp[-\hat{H}(\mathbf{c}) + \int_0^N dt \phi(t, \mathbf{r}) \hat{\rho}(t, \mathbf{r})] \quad (\text{A.4})$$

Now, $Z_M\{\phi\}$ is the partition function of the matrix under the t -dependent external potential function, $\phi(t, \mathbf{r})$. The field theoretical formulation described earlier is readily adapted for (A.4) where the analogous generating function $W_M\{\phi\}$ is defined by a formula like (2.3). The equilibrium probability distribution of the test-chain configuration where the matrix effects are averaged out is governed by the following effective test-chain Hamiltonian:

$$\hat{H}_0(\mathbf{c}_0) - W_M\{\hat{\phi}(\cdot, \cdot; \mathbf{c}_0)\} \quad (\text{A.5})$$

The second term of (A.5) gives rise to various effective interactions among elements of the test chain that are mediated by the matrix, which can be directly obtained by expanding W_M in powers of the following test-chain segment density:

$$\hat{\rho}_0(t_0, \mathbf{r}_0) \equiv \delta(\mathbf{r}_0 - \mathbf{c}_0(t_0)) \quad (\text{A.6})$$

Thus we find

$$\begin{aligned} -W_M\{\hat{\phi}(\cdot, \cdot; \mathbf{c}_0)\} = \\ \sum_{m=1}^{\infty} \frac{1}{m!} \int_0^{N_0} dt_{01} \dots \int_0^{N_0} dt_{0m} \int d\mathbf{r}_{01} \dots \int d\mathbf{r}_{0m} \times \\ U_m(t_{01}, \mathbf{r}_{01}, \dots, t_{0m}, \mathbf{r}_{0m}) \hat{\rho}_0(t_{01}, \mathbf{r}_{01}) \dots \hat{\rho}_0(t_{0m}, \mathbf{r}_{0m}) \end{aligned} \quad (\text{A.7})$$

where

$$\begin{aligned} U_m(t_{01}, \mathbf{r}_{01}, \dots, t_{0m}, \mathbf{r}_{0m}) \equiv \\ (-1)^{m+1} \int_0^N dt_1 \dots \int_0^N dt_m \int d\mathbf{r}_1 \dots \int d\mathbf{r}_m \times \\ v_{t_{01}t_1}(\mathbf{r}_{01} - \mathbf{r}_1) \dots v_{t_{0m}t_m}(\mathbf{r}_{0m} - \mathbf{r}_m) C_m^{\rho}(t_1, \mathbf{r}_1, \dots, t_m, \mathbf{r}_m) \end{aligned} \quad (\text{A.8})$$

and

$$C_m^{\rho}(t_1, \mathbf{r}_1, \dots, t_m, \mathbf{r}_m) \equiv \langle \hat{\rho}(t_1, \mathbf{r}_1) \dots \hat{\rho}(t_m, \mathbf{r}_m) \rangle_c \quad (\text{A.9})$$

$\langle \dots \rangle_c$ denoting the cumulant average over the equilibrium average of the matrix.

As a simple example we consider the two-body interaction between test-chain segments when both the test and matrix chains are homopolymers and thus the segment interaction $v_{t_0 t}(\mathbf{r})$ no longer depends on t_0 and t . The corresponding term of $-W_M$ denoted as $-W_M^{(2)}$ is given by

$$-W_M^{(2)} = \frac{1}{2} \int_0^{N_0} dt_{01} \int_0^{N_0} dt_{02} U_2(\mathbf{c}_0(t_{01}), \mathbf{c}_0(t_{02})) \quad (\text{A.10})$$

where

$$U_2(\mathbf{r}_{01}, \mathbf{r}_{02}) \equiv - \int \int d\mathbf{r}_1 d\mathbf{r}_2 v(\mathbf{r}_{01} - \mathbf{r}_1) v(\mathbf{r}_{02} - \mathbf{r}_2) C_2^T(\mathbf{r}_1, \mathbf{r}_2) \quad (\text{A.11})$$

$$C_2^T(\mathbf{r}_1, \mathbf{r}_2) \equiv \langle \hat{\rho}_T(\mathbf{r}_1) \hat{\rho}_T(\mathbf{r}_2) \rangle_c \quad (\text{A.12})$$

and

$$\hat{\rho}_T(\mathbf{r}) \equiv \int_0^N \hat{\rho}(\mathbf{r}, t) dt \quad (\text{A.13})$$

Thus for the test chain immersed in a homopolymer matrix, $\delta u(\mathbf{r}) \equiv U_2(\mathbf{r}, 0)$ gives a correction to the interaction between two test-chain elements. Then, Fourier transforming both sides of (A.11) where wavy signs are used to denote Fourier transforms, we obtain

$$\delta \tilde{u}(\mathbf{k}) = -\tilde{v}(\mathbf{k})^2 \hat{C}_2^T(\mathbf{k}) \quad (\text{A.14})$$

To proceed further, we employ the small \mathbf{k} form of $\hat{C}_2^T(\mathbf{k})$ given by the random-phase approximation (RPA) as^{8b}

$$\hat{C}_2^T(\mathbf{k}) = (12\rho_0/b^2)(k^2 + \xi^{-2})^{-1} \quad (\text{A.15})$$

$$\xi^{-2} = \frac{12\rho_0}{b^2} \tilde{w}(0) + 2/R_g^2 \quad (\text{A.16})$$

where ρ_0 is the equilibrium monomer number density, b the Kuhn length, R_g the gyration radius of the matrix chain, and $\tilde{w}(\mathbf{k})$ the Fourier transform of the segment interaction potential of matrix chains. In particular, for the athermal case where the test chain and the matrix chains are of the same kind where $v(\mathbf{r}) = w(\mathbf{r})$, we have for $\mathbf{k} \rightarrow 0$

$$\delta \tilde{u}(0) = -\tilde{w}(0) + \frac{2/R_g^2}{(12\rho_0/b^2)\tilde{w}(0) + 2/R_g^2} \tilde{w}(0) \quad (\text{A.17})$$

For very long matrix chains, the second term becomes vanishingly small, resulting in the screening of the potential $w(\mathbf{r})$ with the screening length ξ much shorter than the chain gyration radius.^{8b} (In (A.16) we have kept the second term simply to show the N dependence of ξ .) This result can be readily extended to the case where chains are affinely and uniformly distorted, as in a small volume inside a block copolymer domain. If the stretching ratios of the x direction and the y or z directions are denoted as ϵ_{\parallel} and ϵ_{\perp} , respectively, the result (A.15) remains unchanged if k^2 is replaced by $\epsilon_{\parallel}^2 k_x^2 + \epsilon_{\perp}^2(k_y^2 + k_z^2)$. Thus the screening remains the same as long as ϵ_{\parallel} and ϵ_{\perp} are finite. The situation becomes delicate in block copolymers where ϵ_{\parallel} is $N^{1/6}$ on the average and the screening length in the x direction can become quite large behaving as $\epsilon_{\parallel} \xi \sim N^{1/6} \xi$. The increase of screening length found here is due to the decrease of entropy reduction effects by chain stretching.

Now for the realistic case of a test chain immersed in a domain of the block copolymer system, which consists of mostly one kind of block, say, the A block, the above argument of screening for spatially uniform homopolymer melt must be generalized. The correction δu to $u(\mathbf{r}_{01} - \mathbf{r}_{02})$ now is given by (A.11). That is

$$\delta u(\mathbf{r}, \mathbf{r}') = - \int \int d\mathbf{r} d\mathbf{r}' v(\mathbf{r} - \mathbf{r}') v(\mathbf{r}' - \mathbf{r}) C_2^T(\mathbf{r}, \mathbf{r}') \quad (\text{A.18})$$

Let us now assume that $v(\mathbf{r})$ is short-ranged and both \mathbf{r} and \mathbf{r}' in δu are well inside the same A-rich domain so that their distances from the domain walls are greater than the range of $v(\mathbf{r})$. As we shall see below, $C_2^T(\mathbf{r}, \mathbf{r}')$ is also short-ranged, and hence only the monomer density fluctuations occurring in the A domain under consideration (here denoted as ω_A) need to be included in obtaining $C_2^T(\mathbf{r}, \mathbf{r}')$. Hereafter in this section we omit subscripts A and

superscripts T .

The RPA approximation for $C_2(\mathbf{r}, \mathbf{r}')$ is obtained from the following expression for the free energy functional, $H_2[\rho]$, of the density fluctuation $\delta\rho(\mathbf{r})$ occurring in ω

$$H_2[\rho] = \frac{1}{2} \int \int w(\mathbf{r}-\mathbf{r}') \delta\rho(\mathbf{r}) \delta\rho(\mathbf{r}') d\mathbf{r} d\mathbf{r}' + H_2^G[\rho] \quad (\text{A.19})$$

where the volume integrals are over ω and the second term is the contribution from noninteracting Gaussian-like A-block chains in the mean field $-(1-f)\phi_G(\mathbf{r})$ (see section 3 for ϕ_G). We can write

$$H_2^G[\rho] = \frac{1}{2} \int \int \langle \mathbf{r} | \mathbf{C}_G^{-1} | \mathbf{r}' \rangle \delta\rho(\mathbf{r}) \delta\rho(\mathbf{r}') d\mathbf{r} d\mathbf{r}' \quad (\text{A.20})$$

where \mathbf{C}_G^{-1} is the inverse of the matrix \mathbf{C}_G whose $\mathbf{r}\mathbf{r}'$ element is given by

$$\langle \mathbf{r} | \mathbf{C}_G | \mathbf{r}' \rangle = C_G(\mathbf{r}, \mathbf{r}') \quad (\text{A.21})$$

$C_G(\mathbf{r}, \mathbf{r}')$ being the monomer density correlation of the Gaussian chain system under consideration. Then (A.19) is written as

$$H_2[\rho] = \frac{1}{2} \int \int \langle \mathbf{r} | \mathbf{C}^{-1} | \mathbf{r}' \rangle \delta\rho(\mathbf{r}) \delta\rho(\mathbf{r}') d\mathbf{r} d\mathbf{r}' \quad (\text{A.22})$$

where

$$\mathbf{C}^{-1} \equiv \mathbf{w} + \mathbf{C}_G^{-1} \quad (\text{A.23})$$

and the $\mathbf{r}\mathbf{r}'$ elements of matrices \mathbf{C} and \mathbf{w} are given by $C_2(\mathbf{r}, \mathbf{r}')$ and $w(\mathbf{r}-\mathbf{r}')$, respectively. The expression for C_G is obtained, for instance, in ref 9b as

$$C_G(\mathbf{r}, \mathbf{r}') = n \int dt \int dt' q_{Nt}^-(\mathbf{r}) Q_{tt'}(\mathbf{r}, \mathbf{r}') q_{t'0}^+(\mathbf{r}') / \int d\mathbf{r} \int d\mathbf{r}' Q_{N0}(\mathbf{r}, \mathbf{r}') \quad (\text{A.24})$$

where $Q_{tt'}(\mathbf{r}, \mathbf{r}')$ is the Helfand chain propagator defined in section 3 inside ω (N_A is denoted as N), and

$$q_{Nt}^-(\mathbf{r}) = \int Q_{Nt}(\mathbf{r}', \mathbf{r}) d\mathbf{r}' \quad (\text{A.25})$$

$$q_{t0}^+(\mathbf{r}) = \int Q_{t0}(\mathbf{r}, \mathbf{r}') d\mathbf{r}' \quad (\text{A.26})$$

The integrations with respect to t and t' in (A.24) are over the A-block contour of a chain.

To simplify the analyses, we assume the δ -function-type potentials for $v(\mathbf{r})$ and $w(\mathbf{r})$ like $v_0\delta(\mathbf{r})$, etc. Then (A.18) becomes

$$\begin{aligned} \delta u(\mathbf{r}, \mathbf{r}') &= -v_0^2 C_2(\mathbf{r}, \mathbf{r}') = -v_0^2 \langle \mathbf{r} | (\mathbf{w} + \mathbf{C}_G^{-1})^{-1} | \mathbf{r}' \rangle \\ &= -v_0^2 [w_0^{-1} \delta(\mathbf{r}-\mathbf{r}') - w_0^{-2} \langle \mathbf{r} | \mathbf{C}_G^{-1} | \mathbf{r}' \rangle + \\ &\quad w_0^{-3} \int d\mathbf{r} \langle \mathbf{r} | \mathbf{C}_G^{-1} | \mathbf{r} \rangle \langle \mathbf{r} | \mathbf{C}_G^{-1} | \mathbf{r}' \rangle - \dots] \quad (\text{A.27}) \end{aligned}$$

In order to estimate the size of higher order terms in (A.27), we integrate (A.27) over \mathbf{r}' :

$$\int \delta u(\mathbf{r}, \mathbf{r}') d\mathbf{r}' = -\frac{v_0^2}{w_0} + \frac{v_0^2}{w_0^2} \int \langle \mathbf{r} | \mathbf{C}_G^{-1} | \mathbf{r}' \rangle d\mathbf{r}' + \dots \quad (\text{A.28})$$

The relative sizes of the corrections are then given by powers of the quantity

$$\frac{1}{w_0} \int \langle \mathbf{r} | \mathbf{C}_G^{-1} | \mathbf{r}' \rangle d\mathbf{r}' \quad (\text{A.29})$$

An estimate of this integral is obtained by integrating the following expression with respect to \mathbf{r} and \mathbf{r}'

$$\int \langle \mathbf{r} | \mathbf{C}_G^{-1} | \mathbf{r} \rangle \langle \mathbf{r} | \mathbf{C}_G | \mathbf{r}' \rangle d\mathbf{r} = \delta(\mathbf{r}-\mathbf{r}') \quad (\text{A.30})$$

to get

$$\int d\mathbf{r} \left(\int d\mathbf{r}' \langle \mathbf{r} | \mathbf{C}_G^{-1} | \mathbf{r}' \rangle \right) \left(\int d\mathbf{r}' \langle \mathbf{r}' | \mathbf{C}_G | \mathbf{r} \rangle \right) = V_\omega \quad (\text{A.31})$$

V_ω being the volume of the domain ω . Hence we obtain roughly

$$\int \langle \mathbf{r} | \mathbf{C}_G^{-1} | \mathbf{r}' \rangle d\mathbf{r}' \sim \left(\int \langle \mathbf{r} | \mathbf{C}_G | \mathbf{r}' \rangle d\mathbf{r}' \right)^{-1} \quad (\text{A.32})$$

Now, $\langle \mathbf{r} | \mathbf{C}_G | \mathbf{r}' \rangle$ is nonvanishing over the region where $\mathbf{r}-\mathbf{r}'$ is inside the volume occupied by a single chain. The integral is directly obtained using (A.24) as

$$\begin{aligned} \int C_G(\mathbf{r}, \mathbf{r}') d\mathbf{r}' &= nN \int dt q_{Nt}^-(\mathbf{r}) q_{t0}^+(\mathbf{r}) / \\ &\int d\mathbf{r} q_{Nt}^-(\mathbf{r}) q_{t0}^+(\mathbf{r}) = \rho_0 V_\omega \rho(\mathbf{r}) / n \simeq \rho_0 N \quad (\text{A.33}) \end{aligned}$$

where $\rho(\mathbf{r})$ is the total monomer density at \mathbf{r} which is almost constant equal to ρ_0 . Thus the ratio (A.29) is

$$1/w_0 \rho_0 N \quad (\text{A.34})$$

and is indeed small for large N . The same estimate (A.33) is obtained aside from a numerical factor also for a spatially uniform system of Gaussian chains as one can immediately see by setting \mathbf{k} and $\tilde{w}(0)$ in (A.15) and (A.16) equal to zero.

For $v_0 = w_0$, the smallness of (A.34) implies that the segment interaction $w(\mathbf{r}-\mathbf{r}')$ is practically screened by $\delta u(\mathbf{r}, \mathbf{r}')$ if \mathbf{r} is sufficiently far from \mathbf{r}' , as is the case for isotropic homogeneous polymer melt.⁸ However, we have not been able to estimate the distance $|\mathbf{r}-\mathbf{r}'|$ beyond which screening takes place from our results obtained so far. On the other hand, if we suppose that the melt is almost incompressible, $C_2(\mathbf{r}, \mathbf{r}')$ should be short-ranged and so is its inverse \mathbf{C}^{-1} as well as $\mathbf{C}^{-1} - \mathbf{w}$. Thus the screening is expected to be short-ranged although we have been unable to prove this analytically in RPA.

If we do not use the RPA approximation, the small \mathbf{k} behavior of (A.14) is related to the isothermal compressibility of the matrix χ_T (take the thermodynamic limit $n \rightarrow \infty$ first before taking the limit $\mathbf{k} \rightarrow 0$) as

$$\delta \tilde{u}(0) = -\tilde{v}(0)^2 \rho_0^2 \chi_T \quad (\text{A.35})$$

However, use of such a formula for highly incompressible polymer melts with $v = w$ is limited since expansion in v is no longer appropriate. Here a more detailed treatment of the kind recently advanced by Curro and Schweizer²⁰ may be required.

Appendix B

The classical path that enters (6.15) is the same as (6.8). This implies

$$x_0 = x / \cos \omega t \quad (\text{B.1})$$

and hence

$$\begin{aligned} \tilde{Q}_{N_A t}^A(0x) \tilde{Q}_{t0}^A(xx_0) &= \\ \chi \frac{\omega}{2\pi T} [\sin \omega t \cos \omega t]^{-1/2} \delta(x_0 - x / \cos \omega t) \quad (\text{B.2}) \end{aligned}$$

where χ is still unknown. One can readily verify that the classical action integrals entering the two \tilde{Q} 's in (B.2) cancel each other by virtue of (B.1). The unknown χ is then determined by noting that integration of (B.2) should yield

$$\tilde{Q}_{N_A 0}^A(0x_0) = (\omega / 2\pi T)^{1/2} \quad (\text{B.3})$$

Hence we have

$$\chi = [(2\pi T \tan \omega t) / \omega]^{1/2} \quad (\text{B.4})$$

and

$$\bar{Q}_{N_A t}^A(0x) \bar{Q}_{t0}^A(x x_0) = (\omega/2\pi T)^{1/2} \delta(x - x_0 \cos \omega t) \quad (\text{B.5})$$

Substituting this result into (6.15) and performing double integrations and noting, in view of (B.3)

$$\bar{q}_A = \frac{1}{2} D_A (\omega/2\pi T)^{1/2} \quad (\text{B.6})$$

we find after some algebra

$$(6.15) = \frac{1}{\pi} \ln \frac{1 + [1 - (x/R)^2]^{1/2}}{1 - [1 - (x/R)^2]^{1/2}} \quad (\text{B.7})$$

In obtaining the above result we noted $D/N = D_A/N_A$ and (6.7) and have used the fact that t in the integral is bounded from above by $t(x) = \omega^{-1} \cos^{-1}(x/R)$.

On the other hand, if we carry out the t integration first in (6.15), we obtain

$$(6.15) = \frac{1}{N_A} \int_x^{D_A/2} dx_0 v(x; x_0)^{-1} \quad (\text{B.8})$$

where $v(x; x_0)$ is the same as (6.9) with c replaced by x , and we recover (B.7). If we add a small correction $V(x)$ to the harmonic potential $f_A \phi_G(x)$, the integrand of (B.8) acquires an extra correction factor¹⁴

$$\exp \left[-\frac{1}{T} \int_0^{N_A} dt V(x_0 \cos \omega t) \right] \quad (\text{B.9})$$

If $V(x)$ is so chosen that (B.9) is the same as the Semenov and point distribution (6.12) times R , (B.8) reduces to unity. The actual form of such $V(x)$ was obtained in ref 14 and expressed in (7.6).

Appendix C

Here we consider half of the A-rich domain ($0 \leq x \leq R \equiv (1/2)D_A$) in the classical limit of small T . First we define with $0 \leq x_0 \leq R$

$$\tilde{g}(x_0) \equiv \bar{Q}_{N_A 0}^A(0, x_0) / \bar{q}_A \quad (\text{C.1})$$

where \bar{q}_A is defined by (5.2a) or, here, by

$$\bar{q}_A \equiv \int_0^R \bar{Q}_{N_A 0}^A(0, x_0) dx_0 \quad (\text{C.2})$$

Also we define

$$1/\tilde{v}(x; x_0) \equiv \int_0^{N_A} dt \bar{Q}_{N_A t}^A(0, x) \bar{Q}_{t0}^A(0, x) / \bar{Q}_{N_A 0}^A(0, x_0) \quad (\text{C.3})$$

In the classical limit

$$\bar{Q}_{N_A t}^A(0, x) \bar{Q}_{t0}^A(x, x_0) = \bar{Q}_{N_A 0}^A(0, x_0) \delta(x - c(t; x_0)) \quad (\text{C.4})$$

where $c(t; x_0)$ denotes the classical path determined by

$$\begin{aligned} c(0; x_0) &= x_0 \\ c(N_A; x_0) &= 0 \end{aligned} \quad (\text{C.5})$$

Hence

$$\begin{aligned} 1/\tilde{v}(x; x_0) &= \int_0^{N_A} \delta(x - c(t; x_0)) dt = 1/|\partial c(x; x_0)/\partial t|_{c(t; x_0)=x} \quad 0 \leq x \leq x_0 \\ &= 0 \quad \text{otherwise} \end{aligned} \quad (\text{C.6})$$

Therefore $\tilde{v}(x; x_0)$ is the speed at x of the classical path that started at x_0 , and $\tilde{g}(x_0)$ is the end-point probability distribution of an A-block chain whose junction point is at $x = 0$.

Now the condition (5.6a) becomes in the classical limit using the symmetry

$$\frac{1}{\bar{q}_A} \int_0^{N_A} dt \int_x^R dx_0 \bar{Q}_{N_A t}^A(0, x) \bar{Q}_{t0}^A(x, x_0) = N_A/R \quad (\text{C.7})$$

Using (C.2) and (C.3), this is written as

$$\int_x^R dx_0 \tilde{g}(x_0) / \tilde{v}(x; x_0) = N_A/R \quad (\text{C.8})$$

One can also verify for $0 < x_0 < R$

$$\int_0^{x_0} dx \tilde{v}(x; x_0) = N_A \quad (\text{C.9})$$

The equations like (C.8) and (C.9) appear in ref 5 and express the condition of constant monomer density and the fixed A-block chain contour length, respectively.

The free energy of a single A-block chain, \tilde{h}_A , is given, apart from a small contribution arising from the entropy of end-point distribution, by

$$\tilde{h}_A = \frac{N_A}{R} \int_0^R U(x) dx \quad (\text{C.10})$$

where

$$U(x) \equiv f_A \phi_G(x) \quad (\text{C.11})$$

Using (C.8) and noting that $\partial c(t; x_0)/\partial t$ is in fact negative, (C.10) is transformed into

$$\tilde{h}_A = \int_0^R dx_0 \tilde{g}(x_0) \int_0^{N_A} dt U(c(t; x_0)) \quad (\text{C.12})$$

This is as far as we can go without making any specific choice for the potential $U(x)$.

If we accept the argument that $U(x)$ is taken to be the harmonic potential (6.17) with a small correction, which is important only to produce the correct end-point distribution, $\tilde{g}(x_0)$, we can replace $U(x)$ as well as the path $c(t; x_0)$ by those for the harmonic oscillator. Then the time integral in (C.12) is over $1/4$ of the period of the harmonic oscillator. We can then use the virial theorem to replace the potential energy, $U(c(t; x_0))$, by the kinetic energy, $(1/2)[\partial c(t; x_0)/\partial t]^2$, to obtain

$$\tilde{h}_A = \int_0^R dx_0 \tilde{g}(x_0) \int_0^{N_A} dt \frac{1}{2} [\partial c(t; x_0)/\partial t]^2 \quad (\text{C.13})$$

which is equivalent to (6.5).

References and Notes

- Ohta, T.; Kawasaki, K. *Macromolecules* **1986**, *19*, 2621.
- Kawasaki, K.; Ohta, T.; Kohrogui, M. *Macromolecules* **1988**, *21*, 2972.
- Leibler, L. *Macromolecules* **1980**, *13*, 1602.
- (a) Helfand, E.; Tagami, Y. *J. Chem. Phys.* **1972**, *56*, 3592. Helfand, E. *J. Chem. Phys.* **1975**, *62*, 999. (b) Helfand, E. *Macromolecules* **1975**, *8*, 552. Helfand, E.; Wasserman, Z. R. *Macromolecules* **1976**, *9*, 879.
- Semenov, A. N. *Sov. Phys.-JETP (Engl. Transl.)* **1985**, *61*, 733.
- Here we neglect elastic contributions to $H^S[\psi]$ associated with curvature since $H^S[\psi]$ is similar to that for the incompatible blend. Elasticity associated with curvature of the block copolymer system can arise if $H^L[\psi]$ is also included. See ref 7.
- Kawasaki, K.; Ohta, T. *Physica* **1986**, *139A*, 223.
- (a) de Gennes, P.-G. *Scaling Concepts in Polymer Physics*; Cornell University: Ithaca, NY, 1953. (b) Doi, M.; Edwards, S. F. *The Theory of Polymer Dynamics*; Oxford University Press: New York, 1986.
- (a) Kawasaki, K.; Sekimoto, K. *Physica* **1988**, *143A*, 349. (b) Kawasaki, K.; Sekimoto, K. *Physica* **1988**, *148A*, 361.
- The reviewer reminded us that for the types of morphology having domain walls of finite curvature, the task of obtaining classical approximation for the \bar{Q} 's can be quite wicked due to the presence of a "dead zone". See: Milner, S. T.; Witten, T. A. *J. Phys. (Paris)* **1988**, *49*, 1951.

- (11) Wiegel, F. W. *Introduction to Path-Integral Methods in Physics and Polymer Science*; World Scientific: Singapore, 1986.
- (12) Milner, S. T.; Wittn, T. A.; Cates, M. E. *Macromolecules* 1988, 21, 2610.
- (13) Brout, R. *Phys. Rev.* 1959, 115, 824.
- (14) Milner, S. T.; Wang, Z.-G.; Witten, T. A. *Macromolecules* 1989, 22, 489.
- (15) Viovy, J. L.; Gelbart, W. M.; Ben-Shaul, A. *J. Chem. Phys.* 1987, 87, 4114.
- (16) The quantity $R_A/Z_A^{1/2}$ in Helfand and Wasserman's paper corresponds to $(2T)^{-1/2}(D_A/N_A^{1/2})$ in our notation.
- (17) Witten, T. A.; Leibler, L.; Pincus, P. A., preprint.
- (18) Hohenberg, P.; Kohn, W. *Phys. Rev.* 1964, 136, B864.
- (19) Kohn, W.; Sham, J. *Phys. Rev.* 1965, 140, A1133.
- (20) Schweizer, K. S.; Curro, J. G. *Macromolecules* 1988, 21, 3070, 3082 and the earlier references quoted therein.

Stabilization of Carbazole Radical Cation Formed in Poly(*N*-vinylcarbazole) by Charge Delocalization

Yoshinobu Tsujii, Akira Tsuchida, Yoshihiko Onogi, and Masahide Yamamoto*

Department of Polymer Chemistry, Faculty of Engineering, Kyoto University, Yoshida, Sakyo-ku, Kyoto 606, Japan

Received September 20, 1989; Revised Manuscript Received March 1, 1990

ABSTRACT: The transient absorption spectra (charge-resonance (CR) band) of poly(*N*-vinylcarbazole) (PVCz) and the copolymers of *N*-vinylcarbazole (VCz) with methyl methacrylate and vinyl acetate were measured by laser photolysis to investigate the charge delocalization in the polymers. For the copolymers in which the fraction of VCz (f_{VCz}) is less than 0.4, the CR band appeared at ca. 1800 nm. In the case of $f_{VCz} > 0.5$, the CR band was shifted to longer wavelengths with increasing f_{VCz} and the copolymer with $f_{VCz} = 0.83$ showed the same transient absorption spectrum as PVCz. By considering the sequential distribution of the copolymers, the charge formed in PVCz was found to be delocalized among more than two chromophores. For the copolymer ($f_{VCz} = 0.07$) having no neighboring chromophore interaction, the radical-cation transfer to a series of amines was measured to investigate the free energy change (ΔG) dependence of an electron-transfer rate constant (k_e). The result shows that there is a linear relationship between $\log k_e$ and ΔG . By using this relationship, the stabilization energy of the carbazole radical cation in PVCz was estimated to be 0.5 ± 0.1 eV. This value is larger than that of the carbazole dimer radical cation, i.e., the stabilization by the charge delocalization among more than two chromophores is stronger than that of the dimer radical cation.

Introduction

The stabilization of a radical cation by the interaction with neutral chromophores is one of the most important properties in an electron-transfer reaction of a polymer having a pendant chromophore,¹⁻⁵ and the electronic properties of the dimer radical cation have been investigated for intramolecular systems⁶⁻⁹ and for intermolecular systems¹⁰⁻¹⁵ by ESR, γ -ray-irradiated rigid matrix method, pulse radiolysis, and laser photolysis.

Masuhara et al. showed that the dimeric model compounds, *meso*- and *rac*-2,4-di-*N*-carbazolylpentane (*meso*- and *rac*-DCzPe), form the sandwich dimer radical cation having the fully overlapped conformation of carbazole chromophore and the second dimer radical cation having the partially overlapped one, respectively.⁷ Furthermore, they measured the transient absorption spectrum of a carbazole (Cz) radical cation in poly(*N*-vinylcarbazole) (PVCz) in a visible region and concluded that the measured spectrum for PVCz is a superposition of absorption bands of three kinds of dimer radical cations by the comparison with the absorption spectra for dimeric model compounds.¹⁶

We have studied the stability of the Cz radical cation of PVCz and its dimeric model compounds in a solution by the radical-cation-transfer method^{2,17} and by the charge-resonance band measurement^{3,8} to understand the neighboring chromophore interaction on a radical cation.

Consequently, we found that the stabilization energy is ca. 0.3 eV for the sandwich dimer radical cation and ca. 0.1 eV for the second dimer radical cation by the radical-cation-transfer method² and reported that a Cz radical cation formed in PVCz is more stabilized than the dimer radical cations.^{1,2}

In the present study, we measured transient absorption spectra (charge-resonance band) of a Cz radical cation formed in PVCz and the copolymers of *N*-vinylcarbazole (VCz) with methyl methacrylate (MMA) and vinyl acetate (VAc) by laser photolysis. In the copolymers, the neighboring chromophore interaction of Cz^{•+} is interrupted by the inert comonomer, MMA, and VAc. The relation between the charge-resonance (CR) band and the fraction of VCz in the copolymer shows that the Cz radical cation in PVCz is stabilized by the charge delocalization among more than two chromophores. By the radical-cation-transfer method, the stabilization energy of the Cz radical cation in PVCz was estimated to be 0.5 ± 0.1 eV.

Experimental Section

A. Materials. 1. **Electron Donors (D₁).** *N*-Vinylcarbazole (VCz; Tokyo Kasei Kogyo Co.) was recrystallized from methanol and hexane several times. Poly(*N*-vinylcarbazole) (PVCz) was prepared by a radical polymerization initiated by AIBN in degassed benzene at 60 °C. The molecular weight (\bar{M}_w) was determined to be 8×10^5 by GPC (Toyo Soda HLC 802 UR)